NAVAL POSTGRADUATE SCHOOL
MONTEREY, CALIFORNIA

THESIS

BISTATIC RADAR CROSS SECTION SYNTHESIS FOR RECTANGULAR RESISTIVE SHEETS

by

Uğurcan Şamlı

September 1996

Thesis Advisor: David C. Jenn

19970103 033

DTIC QUALITY INSPECTED 2

REPORT DOCUMENTATION PAGE

Form Approved OMB No. 0704-0188

1. AGENCY USE ONLY *(Leave blank)*	2. REPORT DATE September 1996	3. REPORT TYPE AND DATES COVERED Master's Thesis

4. TITLE AND SUBTITLE BISTATIC RADAR CROSS SECTION SYNTHESIS FOR RECTANGULAR RESISTIVE SHEETS	5. FUNDING NUMBERS
6. AUTHOR(S) Uğurcan Şamlı	

7. PERFORMING ORGANIZATION NAME(S) AND ADDRESS(ES) Naval Postgraduate School Monterey, CA 93943-5000	8. PERFORMING ORGANIZATION REPORT NUMBER

9. SPONSORING/MONITORING AGENCY NAME(S) AND ADDRESS(ES)	10. SPONSORING/MONITORING AGENCY REPORT NUMBER

11. SUPPLEMENTARY NOTES The views expressed in this thesis are those of the author and do not reflect the official policy or position of the Department of Defense or the U.S. Government.

12a. DISTRIBUTION/AVAILABILITY STATEMENT Approved for public release; distribution is unlimited.	12b. DISTRIBUTION CODE

13. ABSTRACT *(maximum 200 words)*

A method of moments solution for the bistatic scattering from planar resistive sheets is presented. The matrix scattering equations are inverted to obtain a rigorous inverse solution that can be applied to the synthesis of radar cross section. Computer calculations for several sheets demonstrate that the synthesized resistivity is in good agreement with the original resistivity.

14. SUBJECT TERMS Radar Cross Section Synthesis			15. NUMBER OF PAGES 84
			16. PRICE CODE

17. SECURITY CLASSIFICATION OF REPORT Unclassified	18. SECURITY CLASSIFICATION OF THIS PAGE Unclassified	19. SECURITY CLASSIFICATION OF ABSTRACT Unclassified	20. LIMITATION OF ABSTRACT UL

NSN 7540-01-280-5500

Standard Form 298 (Rev. 2-89)
Prescribed by ANSI Std. 239-18 298-102

BISTATIC RADAR CROSS SECTION SYNTHESIS
FOR
RECTANGULAR RESISTIVE SHEETS

Uğurcan Şamlı
Lieutenant J.G., Turkish Navy
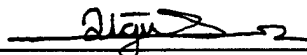Turkish Naval Academy, 1990

Submitted in partial fulfillment
of the requirements for the degree of

MASTER OF SCIENCE IN SYSTEMS ENGINEERING

from the
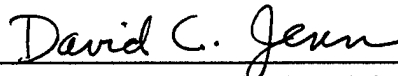
NAVAL POSTGRADUATE SCHOOL
September 1996
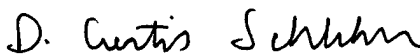
Author: _____
Uğurcan Şamlı

Approved by: _____
David C. Jenn, Thesis Advisor

_____
D. Curtis Schleher, Second Reader

_____
Frederic H. Levien, Chairman
Information Warfare Academic Group

ABSTRACT

A method of moments solution for the bistatic scattering from planar resistive sheets is presented. The matrix scattering equations are inverted to obtain a rigorous inverse solution that can be applied to the synthesis of radar cross section. Computer calculations for several sheets demonstrate that the synthesized resistivity is in good agreement with the original resistivity.

TABLE OF CONTENTS

I. INTRODUCTION

In the early 1970s, stealth technology was revealed to the public. Since then, the term stealth has generally been interpreted to mean "invisible to radar." In reality, however, stealthy targets are not completely invisible. Stealth technology merely reduces the radar cross section (RCS) of the target. The RCS of a target is denoted by σ and may be defined as:

$$\sigma = \frac{\text{Power reflected to receiver per unit solid angle}}{\text{Incident power density} / 4\pi}$$

A great deal of effort is spent to reduce RCS using four basic approaches:

- Target Shaping

- Surface Material Selection and Coatings

- Active Cancellation

- Passive Cancellation

Each of these methods involves trade-offs. For instance, the optimum target shape to achieve reduced RCS may result in aerodynamic problems. Additionally, RCS reduction methods (except for shaping) are usually very narrowband and are effective over limited spatial regions. These factors dictate that RCS reduction methods must be chosen based on the platform's mission and potential threats. The main goal of RCS reduction is to achieve an RCS value below an acceptable threshold over a specified range of frequencies and angles.

The relationship between the electrical characteristics of the material employed and the target's resulting scattered field is a very important concept in RCS reduction (RCSR). The goal of materials selection is to choose a material that yields the smallest reflection of radar waves. The use of radar absorbing materials (RAM) is crucial to RCSR, but because

1

of the complexity of the problem, RCS reduction using RAM has historically been based on intuition and experience.

This thesis examines a method of synthesizing a target's surface material's electrical properties to obtain a specified RCS. Synthesis is a special case of the more general problem of inverse scattering, whereby information on an unknown target is derived from its scattered field. In RCS synthesis, the target shape is usually known; determining the surface material is the primary goal. The synthesis problem can be solved in either the time or frequency domains. This thesis addresses the problem in the frequency domain.

The solution of integral equations provides a basis for obtaining surface impedance information from a target's RCS. In general, both electric and magnetic currents can exist on the surface. Integral equations can be solved by using the method of moments (MM), which is a frequency domain technique. The MM solution employed here requires that the entire structure to be modeled be decomposed into a number of surface patches (subdomains), which must be small compared to the wavelength. There are two approaches to deriving the integral equations for surface impedance synthesis. These are the approximate method and the rigorous method. In the approximate method, the unknown surface impedance is expanded in a series of basis functions with unknown coefficients, and an estimate of the surface current is provided. The rigorous method requires that the coefficients of series expansions for both the impedance and current be determined simultaneously.

Previous works on RCS synthesis have discussed the problem in terms of the approximate method [1 and 2]. The rigorous method is the focus of this thesis. In general, for the rigorous method, a nonlinear set of simultaneous equations must be solved. The present work will be limited to a resistive surface and the target geometry to a flat rectangular plate. Additional boundary conditions will be utilized to solve the synthesis equations for both sets of unknown coefficients. In this limited case the resulting system of equations is linear.

2

Chapter II presents theoretical background required in the formulation and evaluation of the problem. Reflection and transmission coefficients, boundary conditions, and surface impedance concepts are explained. In Chapter III, the RCS of a rectangular resistive sheet is calculated with MM and the RCS synthesis procedure for the rigorous method is developed. Appropriate equations are derived and expressed in matrix form for the bistatic case. In Chapter IV, computer implementations of these synthesis equations are discussed. Chapter V summarizes the results of the synthesis and presents conclusions and recommendations for future research.

II. THEORETICAL BACKGROUND

A.   SURFACE RESISTIVITY

The goal of radar cross section reduction is to eliminate, or at least attenuate significant scattering sources on the target. Thin layers of lossy materials are of special interest in RCSR design, primarily in the treatment of surface waves. Discontinuity boundary conditions are used to mathematically represent thin films. They are the resistive sheet and conductive sheet boundary conditions. The boundary conditions define the relationship between the current and the tangential field components on the surface. A resistive sheet, which is the primary focus of this thesis, is an infinitely thin imperfect electric conductor. Its conductivity is finite, which means $\sigma_c < \infty$, and it does not support a magnetic current ($\vec{J}_{ms} = 0$). For resistivity, the unit ohms per square (Ω / sq) is generally used. This unit is derived from the basic definition of resistance for the special case of length equal to width ($\ell = w$)

$$R_s = \frac{\ell}{\sigma_c t w} = \frac{1}{\sigma_c t} \tag{1}$$

where σ_c is the conductivity of the material per meter and t is the thickness of the material.

There are two limiting values for surface resistance. The first is $R_s = 0$, which represents a perfect electric conductor. The second is $R_s = \infty$, which represents a surface matched to free space.

The boundary conditions may be expressed in general vector form as [1]

$$\hat{n} \times \vec{E}(+) - \hat{n} \times \vec{E}(-) = 0 , \tag{2}$$

$$\hat{n} \times \vec{H}(+) - \hat{n} \times \vec{H}(-) = \vec{J}_s , \tag{3}$$

with:

5

$$\hat{n} \times \left\{ \hat{n} \times \vec{E}(\pm) \right\} = -R_s \vec{J}_s , \tag{4}$$

where $\hat{n}$ is the unit vector normal to the sheet, and is directed to the upper side of the sheet, and $\vec{J}_s$ is the total electric current supported. Plus and minus signs represent upper and lower faces of the sheet, respectively.

The electromagnetic dual of the resistive sheet is the magnetically conductive sheet, which supports only magnetic currents. A combined sheet consisting of resistive and conductive sheets is equivalent to an impedance surface, which is a surface where permittivity and permeability both differ from the surrounding medium [1]. The surface impedance approximation, also known as the Leontovich boundary condition, is:

$$\eta_s = \frac{\vec{E}_{\tan}}{\vec{H}_{\tan}} , \tag{5}$$

where $\vec{E}_{\tan}$ and $\vec{H}_{\tan}$ are the total tangential fields on the surface, and η_s is the surface impedance in ohms [3]. Solution of a scattering problem for the resistive sheet gives the solution for the conductive case by way of the duality principle.

B.   REFLECTION COEFFICIENT

When a traveling wave reaches an interface between two different regions, it will be reflected or transmitted with the relative magnitudes of the two components determined by the impedances of the two regions. The reflection coefficient for a resistive thin film can be derived from the boundary conditions in equations (2), (3), and (4). The geometry is shown in Figure 1. Bistatic scattering for parallel and perpendicular polarizations are investigated separately. Specular reflection can be assumed because the sheet is infinitely thin.

1.   Parallel Polarization

For parallel polarization (TM case), the incident wave is

$$\vec{E}_i = \hat{\theta} E_\theta^i e^{-j\vec{k} \cdot \vec{r}} , \tag{6}$$

where $\vec{k}$ is the incident wave vector. After some mathematical manipulations, the reflection

coefficient is found to be: [1]

$$\Gamma_{TM} = \frac{-\eta_o \cos\theta_i}{2R_s + \eta_o \cos\theta_i} .$$

(7)

The surrounding medium is assumed to be free space with impedance η_0.
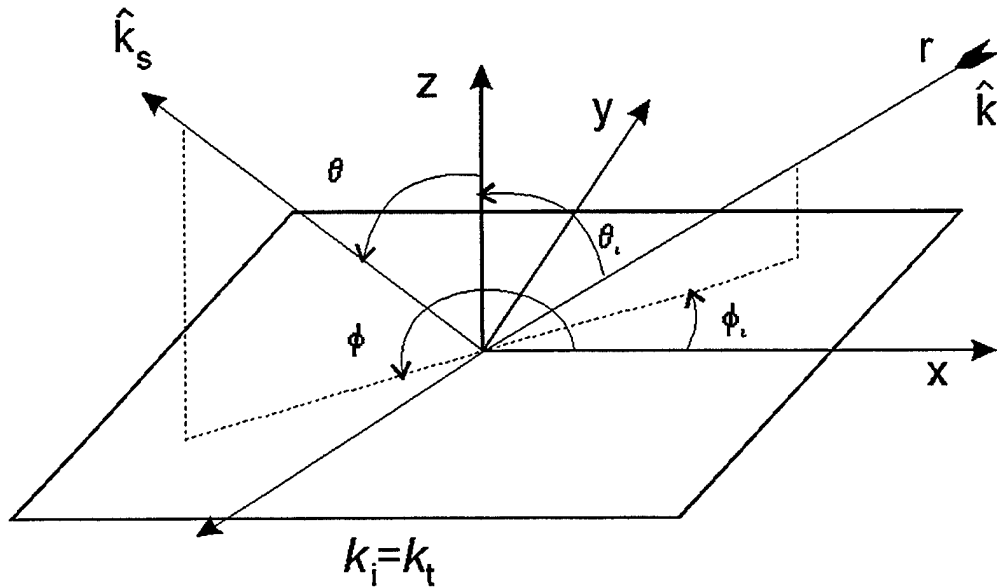

Figure 1. Reflection and Transmission from a Resistive Sheet

2. Perpendicular Polarization

For perpendicular polarization (TE case) the incident wave is:

$$\vec{E}_i = \hat{\phi} \, E_\phi^i e^{-j\vec{k}\cdot\vec{r}}$$

(8)

and the reflection coefficient for the resistive sheet is [1]

$$\Gamma_{TE} = \frac{-\eta_o}{2R_s \cos\theta_i + \eta_o} .$$

(9)

7

C. RADIATION INTEGRALS

The radiation integrals are integral solutions to Maxwell's equations, and are also called Stratton-Chu integrals. They can be derived directly by taking the curl of Maxwell's first two equations, using the vector of Green's theorem, and then integrating [3]. E- and H-fields are determined from current distributions by using the radiation integrals. On a resistive sheet the magnetic currents are zero. The field equations are further simplified when only the far zone fields are of interest.

In the far zone ($kr \gg 1$) and the E- and H-field vectors are orthogonal to each other and the direction of propagation resulting in TEM mode fields. The equations used in this section are derived by Balanis [4]. A rectangular coordinate system is used in formulating the solution for the rectangular sheet problem. The geometry is shown in Figure 2.
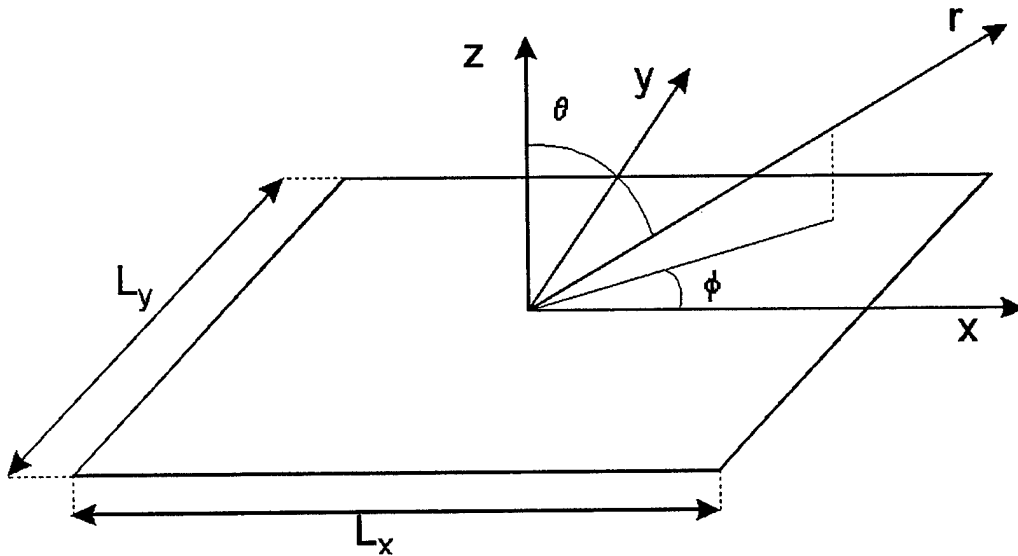

Figure 2. Coordinate System for Scattering from a Planar Rectangular Plate

The far-field spherical components of the E-field are:

$$E_r \cong 0$$

$$E_\theta = -\frac{jke^{-jkr}}{4\pi r}\eta_o N_\theta \, , \qquad (10)$$

and

$$E_\phi = -\frac{jke^{-jkr}}{4\pi r}\eta_o N_\phi \qquad (11)$$

where

$$N_\theta = \iint_s \left[J_x \cos\theta\cos\phi + J_y \cos\theta\sin\phi \right] e^{jkr'\cos\psi} dx'dy' \, , \qquad (12)$$

$$N_\phi = \iint_s \left[-J_x \sin\phi + J_y \cos\phi \right] e^{jkr'\cos\psi} dx'dy' \, , \qquad (13)$$

and

$$r'\cos\psi = x'\sin\theta\cos\phi + y'\sin\theta\sin\phi = x'u + y'v \equiv g . \qquad (14)$$

The direction cosines are

$$u = \sin\theta\cos\phi \, ,$$

$$v = \sin\theta\sin\phi \, ,$$

and

$$w = \cos\theta \, .$$

In order to find scattered fields, the current must be known. The method of moments will be used to find the current. In this approach, the unknown quantity is represented by a series with unknown expansion coefficients. The boundary conditions are imposed to obtain an equation for the current. After the current is found the scattered fields can be obtained from equations (10) and (11). This is referred to as the direct problem, i.e., finding the fields from the currents. Determining the currents from the far field is the inverse or synthesis problem.

9

D.   RCS SYNTHESIS APPROACH

RCS synthesis is a part of a more general problem of inverse scattering. In an inverse scattering problem, the scattering field is known and the objective is to extract current and resistivity information about the target from the scattered field. There are two types of inverse scattering problems: general and restricted. In the general case nothing is known about the target whereas in the restricted case some characteristics of the target are known. The radar cross section synthesis problem falls into the latter case. The target shape is known, but the surface materials and current are to be determined. Synthesis problems can be solved in the time or frequency domains. This thesis deals with synthesis problems in the frequency domain.

At an observation point P, the scattered electric field will be [3]

$$\bar{E}_s(P) = -jk\eta_o \iint_s \left[\bar{J}_s G + \frac{jZ_s}{k}(\hat{n}' \times \bar{J}_s) \times \nabla'G - \frac{\nabla' \cdot \bar{J}_s}{k^2} \nabla'G \right] ds' \qquad (15)$$

where

$$G = \frac{e^{-jkR}}{4\pi R} \qquad \text{and} \qquad R = \left| \bar{r} - \bar{r}' \right|.$$

Primed quantities are associated with the source point; unprimed quantities refer to the observation point. In this equation, $E_s(P)$ is known, but the current and surface impedance are both unknown. This equation can be solved approximately or rigorously. In the first case, the current can be approximated and the equation can be solved for impedance. Equation (15) is sufficient to completely describe the problem. In the second case, both current and impedance must be determined. This requires additional information provided by the following equation: [3]

10

$$\frac{\vec{E}_i(\vec{r})|_{\tan}}{\eta_o} - Z_s(\vec{r})\hat{n}(\vec{r}) \times \vec{H}_i(\vec{r}) = Z_s(\vec{r})\hat{n}(\vec{r}) \times \left[\nabla \times \iint_S \vec{J}_s G ds' \right.$$

$$\left. + jk \iint_S Z_s \left(\hat{n}' \times \vec{J}_s \right) G ds' + \frac{j}{k} \iint_S \nabla' \cdot \left[Z_s \hat{n}' \times \vec{J}_s \right] \nabla G ds' \right] \qquad (16)$$

$$+ \left[jk \iint_S \vec{J}_s G ds' + \frac{j}{k} \iint_S \left(\nabla' \cdot \vec{J}_s \right) \nabla G ds' - \nabla \times \iint_S Z_s \left(\hat{n}' \times \vec{J}_s \right) G ds' \right]_{\tan}$$

Equations (15) and (16) can be solved simultaneously for the current and impedance.

E. METHOD OF MOMENTS

The method of moments is a frequency domain technique. It is used for solving complex integral equations by reducing them to a system of linear equations. The MM technique requires that the entire structure to be modeled be broken down into subdomains. The surface is subdivided to a number of patches with dimensions small compared to the wavelength. Moment methods employ a technique known as the "method of weighted residuals." Actually, the terms method-of-moments and method-of-weighted-residuals are synonymous [5].

The MM technique is popular because it can be applied to arbitrary bodies. Furthermore, integral equations are reduced to a set of linear equations, which are conveniently solved by using matrix algebra. The size of the matrix is directly related to the electrical size of the body. Large bodies result in large matrices, which affects computation time, and limits the size of the targets that can be handled in practice.

The first step in MM for the direct problem is to represent the current by a series with unknown expansion coefficients. For a rectangular resistive plate in the xy plane, one possible representation for the current is:

$$\vec{J}_s(x',y') = \sum_n \left(I_n^x \vec{J}_n^x + I_n^y \vec{J}_n^y \right) . \qquad (17)$$

11

The vectors $\bar{J}_n^x$ and $\bar{J}_n^y$ are the expansion or the basis functions, which are complex in general. Selection of the basis functions is very important. They should be mathematically convenient – in other words, easy to integrate and differentiate. They should also be consistent with the behavior of the current to provide fast convergence [3]. The expansion scheme for the currents can be seen in Figure 3. Two basis functions span each rectangular subsection: one x-directed and a second y-directed. These two orthogonal basis functions are sufficient to uniquely define all possible current vectors on the patch.
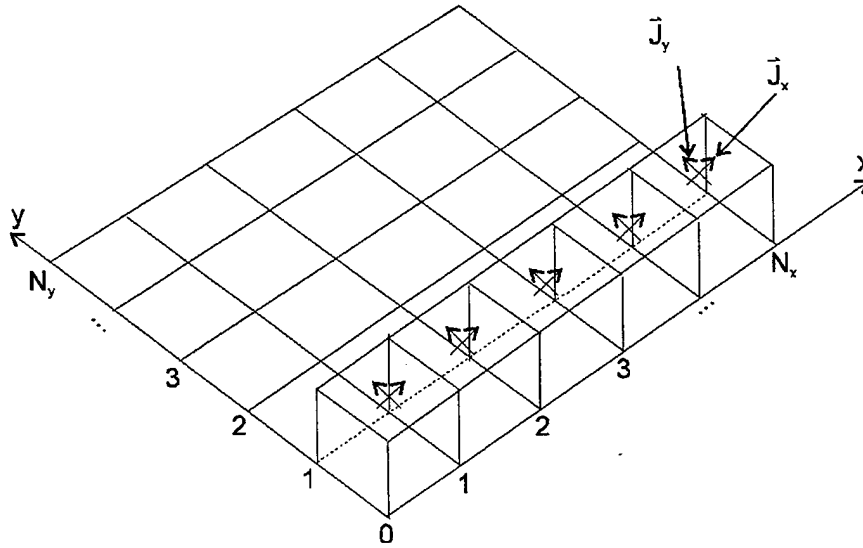

Figure 3. Three-dimensional View of Pulse Basis functions for the Currents $\bar{J}_x$ and $\bar{J}_y$

III. FORMULATION AND SOLUTION

A. RCS OF A RESISTIVE SHEET USING THE METHOD OF MOMENTS

In this section, the scattered field and radar cross section of a resistive sheet is calculated for the bistatic case. This direct problem solution is used to generate and validate the synthesis procedure. A constant resistivity is assumed on each patch, and the method of moments is used to find the current distribution on the plate. Rectangular patches and nonoverlapping pulse basis functions are used for calculations. After the synthesis procedure, the resulting resistivity is compared with the original resistivity to verify the synthesis equations.

The resistive sheet lies in the xy plane. The incident wave is assumed to be a planar wave, and it contains both parallel and perpendicular components [3],

$$\vec{E}^i = \left(\hat{\theta} E_\theta^i + \hat{\phi} E_\phi^i\right)e^{-j\vec{k}\cdot\vec{r}} = \left(\hat{x} E_x^i + \hat{y} E_y^i\right)e^{-j\vec{k}\cdot\vec{r}} \tag{18}$$

where,

$$-j\vec{k}\cdot\vec{r} = jk\left[x\sin\theta_i\cos\phi_i + y\sin\theta_i\sin\phi_i + z\cos\theta_i\right] \tag{19}$$

and,

$$E_x^i = E_\theta^i \cos\theta_i \cos\phi_i - E_\phi^i \sin\phi_i$$
$$E_y^i = E_\theta^i \cos\theta_i \sin\phi_i + E_\phi^i \cos\phi_i \tag{20}$$

The resistive sheet integral equation is solved to find the current distribution on the surface [3],

$$\vec{E}_i(\vec{r})\bigg|_{tan} = R_s\vec{J}_s + \left\{jk\eta_0 \iint_s \vec{J}_s G ds' + \frac{jk}{\eta_0}\nabla\left[\nabla\bullet\iint_s \vec{J}_s G ds'\right]\right\}\bigg|_{tan} \tag{21}$$

13

The unknown current is expanded into a series using equation (17), which can be written in the following manner:

$$\bar{J}_s = J_x \hat{x} + J_y \hat{y} = \hat{x} \sum_n^N I_n^x \frac{p_n(x',y')}{\Delta y} + \hat{y} \sum_n^N I_n^y \frac{p_n(x',y')}{\Delta x} \quad (22)$$

The quantities Δx and Δy are defined in Figure 4, and $p_n(x',y')$ is the pulse function

$$p_n(x',y') = \begin{cases} 1 & , \text{ if } x' \text{ and } y' \text{ on patch } n. \\ 0 & , \text{ else} \end{cases} \quad (23)$$

The method of moments is initiated by inserting equation (22) into (21). At this point a set of testing or weighting functions are defined. The weighting functions describe how the boundary conditions are enforced [6]. These functions are generally chosen to be the complex conjugate of the basis functions ($\bar{W} = \bar{J}^*$), which is known as "Galerkin's Method" [1]. Weighting functions for this case are [7],

$$\bar{W} = \bar{W}_x \hat{x} + \bar{W}_y \hat{y} \quad (24)$$

where,

$$\bar{W}_x = \hat{x} \sum_m^N \frac{p_m(x,y)}{\Delta y} \quad (25)$$

$$\bar{W}_y = \hat{y} \sum_m^N \frac{p_m(x,y)}{\Delta x} \quad (26)$$

Both sides of the equation (21) are multiplied with these weighting functions and integrated. In terms of expansion and weighting functions, the integral equation (equation 21) takes the form

$$\iint_s \bar{E}_i \bullet \bar{W} ds = \iint_s R_s \bar{J}_s \bullet \bar{W} ds + jk\eta_0 \iint_s ds \iint_{s'} ds' \left[\bar{J}_s \bullet \bar{W} - \frac{1}{k^2} (\nabla \bullet \bar{W})(\nabla' \bullet \bar{J}_s) \right] \quad (27)$$

14

Equation (27) can be separated into two equations, one associated with the x components and the second with the y components. The derivatives of the pulse functions are approximated by δ functions as shown in Figure 4. The x component of equation (27) becomes,

$$\delta\left(x - x_n^-, y\right)$$

$$\delta\left(x, y - y_n^-\right)$$

$$\left(x_n, y_n\right) \quad \frac{\Delta y}{2} \quad y$$

$$x_n^\pm = x_n \pm \frac{\Delta x}{2}$$

$$\frac{\Delta x}{2}$$

$$y_n^\pm = y_n \pm \frac{\Delta y}{2}$$

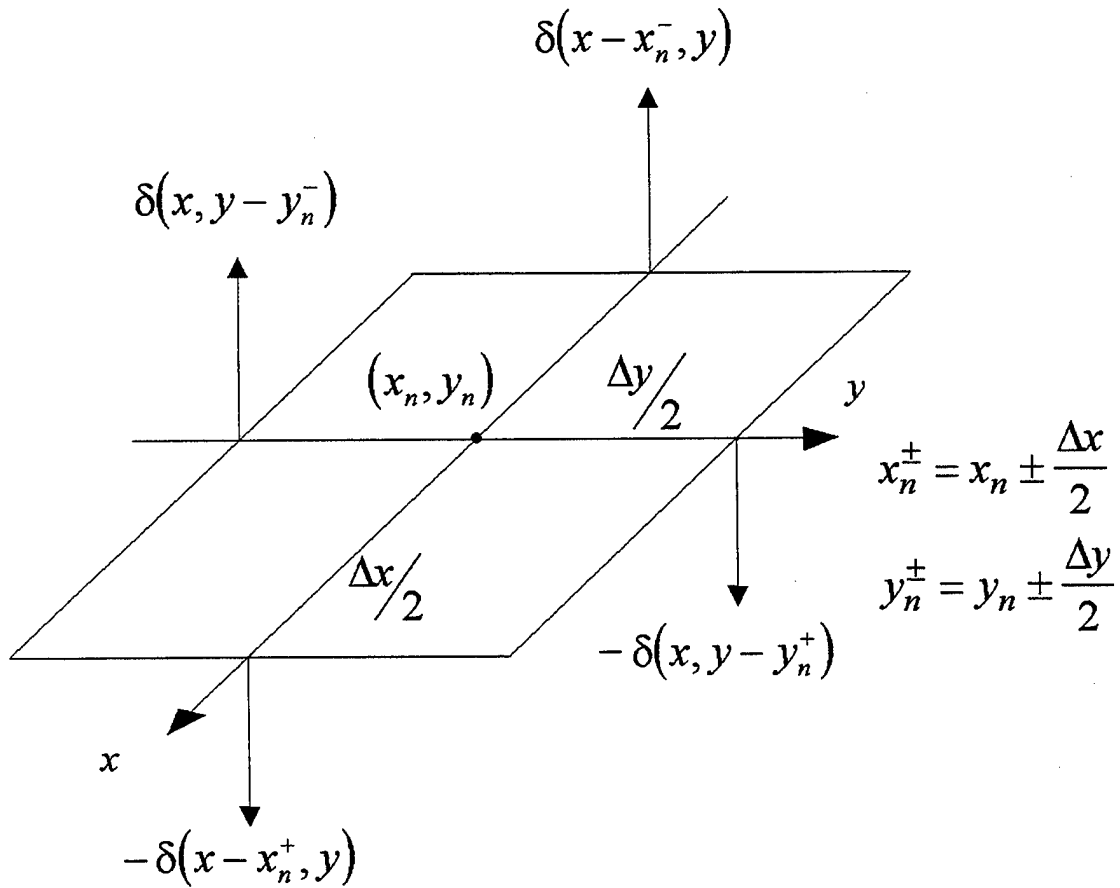$$-\delta\left(x, y - y_n^+\right)$$

$$x$$

$$-\delta\left(x - x_n^+, y\right)$$

Figure 4. Pulse Function Derivatives for a Patch [7].

15

$$\iint_s E_x e^{-j\vec{k}\cdot\vec{r}} \frac{p_m(x,y)}{\Delta y} ds = \iint_s R_s \left(\sum_n I_n^x \frac{p_n(x,y)}{\Delta y} \right) \frac{p_m(x,y)}{\Delta y} ds$$

$$+ jk\eta_0 \iint_s ds \iint_{s'} ds' \left\{ \left(\sum_n \frac{p_n(x',y')}{\Delta y} \right) \frac{p_m(x,y)}{\Delta y} - \frac{1}{k^2} \left[\frac{1}{\Delta y} \left\{ \delta\left(x - x_m^-, y\right) \right. \right. \right.$$

(28)

$$\left. -\delta\left(x - x_m^+, y\right) \right\} \left\{ \sum_n \left[\frac{I_n^x}{\Delta y} \left(\delta\left(x - x_n^-, y\right) - \delta\left(x - x_n^+, y\right) \right) + \frac{I_n^y}{\Delta x} \left(\delta\left(x, y - y_n^-\right) \right. \right. \right.$$

$$\left. \left. \left. \left. -\delta\left(x, y - y_n^+\right) \right) \right] \right\} \right] \right\} G(x,x',y,y').$$

A similar equation can be obtained by testing with the y-directed weighting functions,

$$\iint_s E_y e^{-j\vec{k}\cdot\vec{r}} \frac{p_m(x,y)}{\Delta x} ds = \iint_s R_s \left(\sum_n I_n^x \frac{p_n(x,y)}{\Delta x} \right) \frac{p_m(x,y)}{\Delta x} ds$$

$$+ jk\eta_0 \iint_s ds \iint_{s'} ds' \left\{ \left(\sum_n \frac{p_n(x',y')}{\Delta x} \right) \frac{p_m(x,y)}{\Delta x} - \frac{1}{k^2} \left[\frac{1}{\Delta x} \left\{ \delta\left(x, y - y_m^-\right) \right. \right. \right.$$

(29)

$$\left. -\delta\left(x, y - y_m^+\right) \right\} \left\{ \sum_n \left[\frac{I_n^x}{\Delta y} \left(\delta\left(x' - x_n^-, y'\right) - \delta\left(x' - x_n^+, y'\right) \right) + \frac{I_n^y}{\Delta x} \left(\delta\left(x', y' - y_n^-\right) \right. \right. \right.$$

$$\left. \left. \left. \left. -\delta\left(x', y' - y_n^+\right) \right) \right] \right\} \right] \right\} G(x,x',y,y').$$

16

Now define the following quantities,

$$G_{mn}^{xx} = \frac{jk\eta_0}{\Delta y^2} \iint\limits_{s_m} dx\,dy \iint\limits_{s_n} dx'\,dy'\, G(x,x',y,y')$$ (30)

$$Q_{mn}^{xx} = \frac{-j\eta_0}{k\Delta y^2} \int\limits_{\Delta y_m} dy \int\limits_{\Delta y_n} dy' \left\{ G\left(x_m^-, x_n^-, y, y'\right) - G\left(x_m^-, x_n^+, y, y'\right) \right.$$
$$\left. - G\left(x_m^+, x_n^-, y, y'\right) + G\left(x_m^+, x_n^+, y, y'\right) \right\}$$ (31)

$$Q_{mn}^{xy} = \frac{-j\eta_0}{k\Delta y\Delta x} \int\limits_{\Delta y_m} dy \int\limits_{\Delta x_n} dx' \left\{ G\left(x_m^-, x', y, y_n^-\right) - G\left(x_m^-, x', y, y_n^+\right) \right.$$
$$\left. - G\left(x_m^+, x', y, y_n^-\right) + G\left(x_m^+, x', y, y_n^+\right) \right\}$$ (32)

$$\mathcal{Z}_m^x = \iint\limits_{sm} \frac{R_{sm}}{\Delta y}\,ds = \begin{cases} R_{sm}\dfrac{\Delta x}{\Delta y} & ,\ \text{if } m = n \\ 0 & ,\ \text{if } m \neq n \end{cases}$$ (33)

$$V_n^x = E_x^i \Delta x\,\text{sinc}\!\left(\frac{k\Delta x u_i}{2}\right)\text{sinc}\!\left(\frac{k\Delta y v_i}{2}\right) e^{jk(x_n u_i + y_n v_i)}$$ (34)

$$G_{mn}^{yy} = \frac{jk\eta_0}{\Delta x^2} \iint\limits_{sm} dx\,dy \iint\limits_{sn} dx'\,dy'\, G(x,x',y,y')$$ (35)

$$Q_{mn}^{yy} = \frac{-j\eta_0}{k\Delta x^2} \int\limits_{\Delta y_m} dx \int\limits_{\Delta y_n} dx' \left\{ G\left(x, x', y_m^-, y_n^-\right) - G\left(x, x', y_m^-, y_n^+,\right) \right.$$
$$\left. - G\left(x, x', y_m^+, y_n^-\right) + G\left(x, x', y_m^+, y_n^+\right) \right\}$$ (36)

17

$$Q_{mn}^{yx} = \frac{-j\eta_0}{k\Delta x\Delta y} \int_{\Delta x_m} dx \int_{\Delta y_n} dy' \left\{ G\left(x, x_n^-, y_m^-, y'\right) - G\left(x, x_n^+, y_m^-, y'\right) \right.$$

$$\left. - G\left(x, x_n^-, y_m^+, y'\right) + G\left(x, x_n^+, y_m^+, y'\right) \right\} \tag{37}$$

$$\mathcal{J}_m^y = \begin{cases} R_{sm}\dfrac{\Delta y}{\Delta x} & , \text{ if } m = n \\ 0 & , \text{ if } m \neq n \end{cases} \tag{38}$$

$$V_n^y = E_y^i \Delta y \, \text{sinc}\left(\frac{k\Delta x u_i}{2}\right) \text{sinc}\left(\frac{k\Delta y v_i}{2}\right) e^{jk\left(x_n u_i + y_n v_i\right)} \tag{39}$$

Using equations (30)-(39), equation (28) and equation (29) can be cast in matrix form :

$$\begin{bmatrix} \mathbf{V}^x \\ \mathbf{V}^y \end{bmatrix} = \begin{bmatrix} \mathcal{J}^{\,x} & \\ & \mathcal{J}^{\,y} \end{bmatrix} \begin{bmatrix} \mathbf{I}^x \\ \mathbf{I}^y \end{bmatrix} + \begin{bmatrix} \mathbf{G}^{xx} + \mathbf{Q}^{xx} & \mathbf{Q}^{xy} \\ \mathbf{Q}^{yx} & \mathbf{G}^{yy} + \mathbf{Q}^{yy} \end{bmatrix} \begin{bmatrix} \mathbf{I}^x \\ \mathbf{I}^y \end{bmatrix} \tag{40}$$

For the synthesis problem, the number of unknowns in this equation is $4N$ where N is the number of expansion terms. There are $2N$ current coefficients and $2N$ resistivity coefficients in general. If the material is isotropic then $\mathcal{J}^x = \mathcal{J}^y$ and the number of unknown resistivity coefficients is just N. For the direct problem the number of unknowns is only $2N$.

The integrals appearing in the above equations must be evaluated numerically. To reduce the computer run time, the following approximation can be applied [3],

$$\int_{x_m - \frac{\Delta}{2}}^{x_m + \frac{\Delta}{2}} f(x, x') dx \cong \Delta \, f(x_m, x') \tag{41}$$

With this approximation, the impedance matrix elements in equations (31), (32), (36) and (37) are

$$Q_{mn}^{xx} \cong \frac{-j\eta_0}{k} \left\{ G\left(x_m^-, x_n^-, y_m, y_n\right) - G\left(x_m^-, x_n^+, y_m, y_n\right) \right.$$

$$\left. - G\left(x_m^+, x_n^-, y_m, y_n\right) + G\left(x_m^+, x_n^+, y_m, y_n\right) \right\} \tag{42}$$

18

$$Q_{mn}^{xy} \cong \frac{-j\eta_0}{k} \left\{ G\left(x_m^-, x_n, y_m, y_n^-\right) - G\left(x_m^-, x_n, y_n, y_n^+\right) \right.$$
$$\left. - G\left(x_m^+, x_n, y_m, y_n^-\right) + G\left(x_m^+, x_n, y_m, y_n^+\right) \right\} \tag{43}$$

$$Q_{mn}^{yx} \cong \frac{-j\eta_0}{k} \left\{ G\left(x_m, x_n^-, y_m^-, y_n\right) - G\left(x_m, x_n^-, y_m^+, y_n\right) \right.$$
$$\left. - G\left(x_m, x_n^+, y_m^-, y_n\right) + G\left(x_m, x_n^+, y_m^+, y_n\right) \right\} \tag{44}$$

$$Q_{mn}^{yy} \cong \frac{-j\eta_0}{k} \left\{ G\left(x_m, x_n, y_m^-, y_n^-\right) - G\left(x_m, x_n, y_m^-, y_n^+\right) \right.$$
$$\left. - G\left(x_m, x_n, y_m^+, y_n^-\right) + G\left(x_m, x_n, y_m^+, y_n^+\right) \right\} \tag{45}$$

Note that in all of these equations, the Green's functions in the integrands can become singular for the self term because both the source and the test points lie on the same segment. This problem can be solved by moving the test point off the patch axis [3]. For example, when integrating in x or x',

$$R = \sqrt{(x - x')^2 + (y - y')^2 + a_y^2} \tag{46}$$

and when integrating in y or y',

$$R = \sqrt{(x - x')^2 + (y - y')^2 + a_x^2} \tag{47}$$

In this case, an equivalent radius of the patch is used :

$$a_x \cong 0.225 \, \Delta x \qquad a_y \cong 0.225 \, \Delta y \tag{48}$$

Equation (40) provides a means of solving the direct problem by plugging the resulting current coefficients into the far-field radiation integrals. The current coefficients can be obtained if the incident field and resistivity are known. The scattered field at an observation point (θ_s, ϕ_s) is computed by integrating the current. The current coefficients

19

that occur in the scattering equations are the same for all observation angles, because the same incident field determines these coefficients. After integrating, the scattered electric field has the following form:

$$\bar{E}_s = \frac{-jk\eta_0}{4\pi r}e^{-jkr}\left[\left(\hat{x}\sum_{n=1}^{N}I_n^x\Delta x\,\mathrm{sinc}\left(\frac{k\Delta x u_s}{2}\right)\mathrm{sinc}\left(\frac{k\Delta y v_s}{2}\right)e^{jkg}\right)\right.$$

$$\left.+\left(\hat{y}\sum_{n=1}^{N}I_n^y\Delta y\,\mathrm{sinc}\left(\frac{k\Delta x u_s}{2}\right)\mathrm{sinc}\left(\frac{k\Delta y v_s}{2}\right)e^{-jkg}\right)\right] \qquad (49)$$

$$\equiv \hat{x}E_x^s + \hat{y}E_y^s$$

where:

$$g = x_n u_s + y_n v_s$$
$$= x_n\sin\theta_s\cos\phi_s + y_n\sin\theta_s\sin\phi_s$$

Finally, the complete expression for the θ- and φ- components of the scattered electric field is:

$$E_\theta^s = E_x^s\cos\theta_s\cos\phi_s + E_y^s\cos\theta_s\sin\phi_s \qquad (50)$$

$$E_\phi^s = -E_x^s\sin\phi_s + E_y^s\cos\phi_s \qquad (51)$$

From the definition of the radar cross section for a three-dimensional target [1],

$$\sigma = \lim_{r\to\infty}\left[4\pi r^2\frac{|\bar{E}_s|^2}{|\bar{E}_i|^2}\right] \qquad (52)$$

and the corresponding radar cross section for the θ- and φ- components of the scattered electric field for a unit plane wave are

$$\sigma_{\theta\theta} = \frac{k^2\eta_0^2}{4\pi}\left[E_\theta^{\;s}\right]^2 \qquad (53)$$

$$\sigma_{\phi\theta} = \frac{k^2\eta_0^2}{4\pi}\left[E_\phi^{\;s}\right]^2. \qquad (54)$$

20

The first subscript on σ denotes the polarization of the scattered field, whereas the second one denotes the polarization of the incident wave.

B.   SYNTHESIS FORM OF THE SCATTERING EQUATIONS

The resistivity of the rectangular plate can be determined rigorously by expanding both current and resistivity into series and solving for the expansion coefficients. For this purpose, the scattered electric field is found using the formulation in the previous section. Because the sinc functions in equations (34) and (39) are periodic in direction cosine space (DCS), it is convenient to work in DCS (Figure 5). There are two approaches sampling the RCS in DCS. The first is to choose the observation points entirely inside of the unit circle. The second is to include observation points outside of the unit circle. The first approach makes physical sense because all observation directions are points in real space. Directions outside of the unit circle correspond to complex angles. However, the first method is restrictive in the number of observation points, because they must be equal to the number of subdomains on the plate to obtain a square matrix that can be solved by inversion. The computer program which calculates and plots RCS in DCS is presented in the Appendix.

In synthesizing the plate resistivity the far-field pattern is given. It is known that a resistive sheet does not support magnetic currents, and the far-field is related to the electric currents on the sheet by

$$\bar{E}_s(P) = -jk\eta_0 \iint_s \bar{J}_s G ds'$$ (55)

P denotes an observation point in the direction (r, θ, ϕ) or (x, y, z). On the surface of the sheet, equation (21) still holds, and in this equation resistivity and current are not independent of each other. These two quantities are related at every point on the surface of the sheet by the tangential component of the electric field as indicated in equation (4).

Equations (21) and (55) can be solved simultaneously for the current and resistivity. For the current expansion equation (22) is used, and for the resistivity,

$$R_s = \sum_n^N R_n p_n\left(x',y'\right).\tag{56}$$

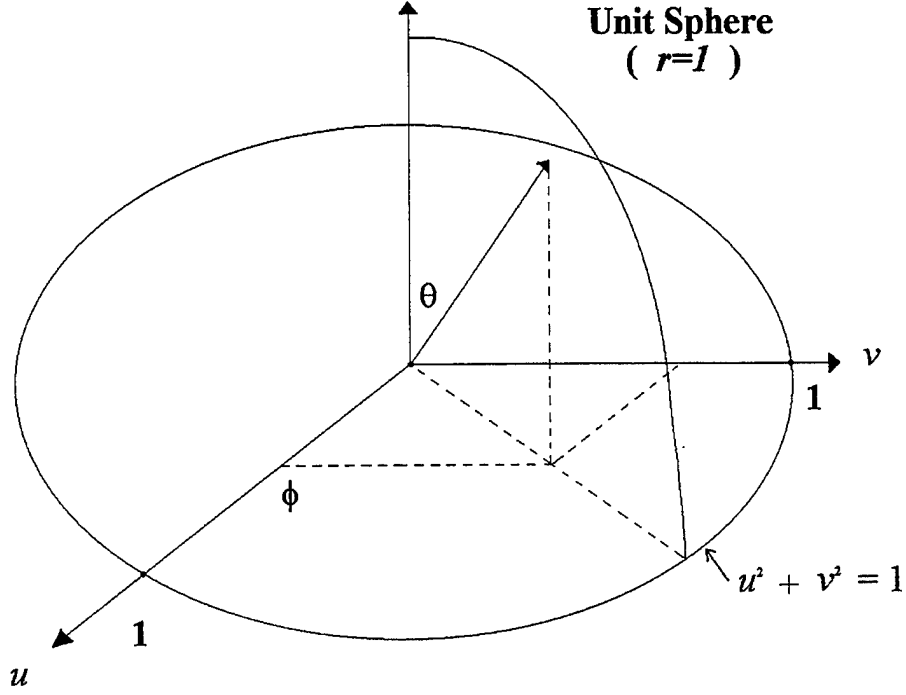

Unit Sphere
(r=1)

Figure 5. Direction Cosine Space (DCS) .

The resistivity is assumed to be constant on each patch. Equation (22) is plugged into the equation (55), and after integration,

$$\vec{E}_s\left(P_m\right) = -jk\eta_0 \frac{e^{-jkr}}{4\pi r} \sum_{n=1}^{N}\left(\frac{I_n^x}{\Delta y}\hat{x} + \frac{I_n^y}{\Delta x}\hat{y}\right)F_n\left(u_m,v_m\right)\tag{57}$$

where the last factor in the equation is

$$F_n\left(u_m,v_m\right) = e^{jk\left(x_n u_m + y_n v_m\right)}\Delta x\Delta y\,\mathrm{sinc}\left(\frac{k\Delta x u_m}{2}\right)\mathrm{sinc}\left(\frac{k\Delta y v_m}{2}\right)\tag{58}$$

22

Equation (57) can be solved for the unknown current coefficients given a set of $m =$ $1,2,....,N$ scattered field values. In matrix form, equation (57) is

$$\mathbf{E}_s^x = \frac{\mathbf{F}}{\Delta y}\mathbf{I}^x \qquad \mathbf{E}_s^y = \frac{\mathbf{F}}{\Delta x}\mathbf{I}^y \qquad (59)$$

These two equations can be combined and put into the following form :

$$\begin{bmatrix} \mathbf{E}_s^x \\ \mathbf{E}_s^y \end{bmatrix} = \begin{bmatrix} \mathbf{F}\!\!\diagup\!\!\Delta y & \\ & \mathbf{F}\!\!\diagup\!\!\Delta x \end{bmatrix} \begin{bmatrix} \mathbf{I}^x \\ \mathbf{I}^y \end{bmatrix} \qquad (60)$$

In equation (60), the only unknowns are the $\mathbf{I}^x$ and $\mathbf{I}^y$ coefficients, and they can be found by simple matrix algebra. After these coefficients are found, they are plugged into the resistive sheet integral equation (equation (21)) to find the resistivity coefficients in equation (56).

$$\begin{bmatrix} \mathbf{V}^x \\ \mathbf{V}^y \end{bmatrix} = \begin{bmatrix} \mathbf{\zeta}^x & \\ & \mathbf{\zeta}^y \end{bmatrix} \begin{bmatrix} \mathbf{I}^x \\ \mathbf{I}^y \end{bmatrix} + \begin{bmatrix} \mathbf{Z}^{xx} & \mathbf{Z}^{xy} \\ \mathbf{Z}^{yx} & \mathbf{Z}^{yy} \end{bmatrix} \begin{bmatrix} \mathbf{I}^x \\ \mathbf{I}^y \end{bmatrix} \qquad (61)$$

There are $4N$ rows in equation (61). In an isotropic resistivity case, there are $3N$ unknowns because the terms $\mathbf{\zeta}^x$ and $\mathbf{\zeta}^y$ in equation (61) are same. Rearranging equation (61)

$$\begin{bmatrix} \mathbf{\zeta}^x & \\ & \mathbf{\zeta}^y \end{bmatrix} \begin{bmatrix} \mathbf{I}^x \\ \mathbf{I}^y \end{bmatrix} = \begin{bmatrix} \mathbf{V}^x \\ \mathbf{V}^y \end{bmatrix} - \begin{bmatrix} \mathbf{Z}^{xx} & \mathbf{Z}^{xy} \\ \mathbf{Z}^{yx} & \mathbf{Z}^{yy} \end{bmatrix} \begin{bmatrix} \mathbf{I}^x \\ \mathbf{I}^y \end{bmatrix} \qquad (62)$$

The matrix operations on the right hand side yield a column vector. The elements of the column vector are $\zeta_m^x I_m^x$ and $\zeta_m^y I_m^y$ and since I_m^x and I_m^y are known, the resistivity can be found by element-wise division.

IV.   COMPUTER IMPLEMENTATION AND RESULTS

A.   INTRODUCTION

In this chapter, the computer coding of the RCS synthesis formulas is described and numerical results are presented for a flat resistive sheet. The results of three investigations are included :

1. Verification of the MM solution for rectangular patches and pulse basis functions.

2. Verification of the synthesis equations derived in Chapter III and a parametric study of convergence.

3. Sampling requirements.

B.   VALIDATION OF THE RECTANGULAR PATCH CODE

The rectangular patch code based on pulse expansion functions developed in Chapter III was programmed in MATLAB. Computed results were compared to a MM code named PATCH [9]. Typical results are shown in Figures 6 through 10. The two codes give essentially the same RCS as expected. The agreement is within 2 dB down to the -40 dB level when the two codes are converged.

Validation of the rectangular patch code is important because many of the same subroutines and functions are used in the synthesis program. Furthermore, the output of this program is used as the input for initializing the synthesis process. Figures 11 and 12 show two dimensional plots of the RCS. The corresponding electric field values are used to fill the vector V in Equation (40).

C.   VERIFICATION OF THE SYNTHESIS EQUATIONS

The synthesis equations and computer codes are validated by the following process :

1. Compute the scattered field for a plate with known surface resistivity.

25

2. Use the scattered field from step 1 in the synthesis procedure.

3. Compare the synthesized resistivity in step 2 to the original resistivity used in step 1. In principle the difference should be zero. However, because of numerical and sampling errors, the residual will not be exactly zero, but some small (and hopefully negligible) value.

The difference between the original and synthesized resistivity ΔR_s is defined by

$$\Delta R_s = R_{sy} - R_{so}$$

where

R_{so} = Original resistivity used to compute the electric field values.

R_{sy} = Synthesized resistivity.

For $R_{so} = 377$, $\Delta R_s \leq 10^{-12}$ as shown in Figure 13. For $R_s = 10$, ΔR_s is as large as 0.06 as illustrated in Figure 14. Similar results are shown in Figures 15 through 19. The lower plate resistivity supports surface waves which increase the size of the off-diagonal elements in Z relative to the size of the diagonal elements. This leads to increased roundoff error. The number of field (RCS) samples N_u and N_v are equal, and they include the points outside of the visible region, which is the second approach as described in Chapter III-B. The number of patches are $N_x = N_u$ and $N_y = N_v$. All of the visible region field points were in the backscatter (rear) hemisphere. Including the points outside the visible region affects the accuracy of the computation and causes some poorly conditioned matrices. However, the error resulting from this approach is not significant. In all cases the residual resistivity was less than 0.6 percent.

D.   SAMPLING REQUIREMENTS

Computer memory and execution time are very important limitations in the scattering and synthesis computations. Reducing computer run time depends on reducing the size of the matrices (especially impedance matrix), and consequently minimizing the number of patches. Thus a guideline for the minimum number of subdomains which gives computationally accurate results is necessary to minimize the computer run time.

For the synthesis calculation the continuous scattered field is sampled just as a continuous time function is sampled in a digital communication system. Therefore the same sampling requirements apply. If the frequency content of the scattered field is plotted, the minimum sampling rate must be at least twice the highest frequency [3]. To obtain the frequency content a two-dimensional discrete Fourier transform (DFT) is performed on the scattered electric field values, which are computed in sufficiently large number. The computation is performed in DCS because most RCS patterns are highly periodic in DCS and thus the number of sampling points is smaller. If N_u and N_v are the number of sampling points in the u and v coordinates, then the sampling intervals are $2/N_u$ and $2/N_v$. This represents π radians in visible space, and hence the scaling of the u and v axes upon returning from the FFT is $2/N_u \Delta u$ and $2/N_v \Delta v$, respectively.

In Figures 20 through 23, frequency information for $1\lambda \times 1\lambda$ and $3\lambda \times 3\lambda$ plates is plotted. The FFT is performed on the center row of the two-dimensional scattered electric field matrix to illustrate the frequency content in one coordinate. The magnitude of this transform is plotted with respect to the number of cycles in DCS in Figures 20 and 22. The result of a two-dimensional FFT performed on the whole E-field matrix is plotted with respect to the number of cycles in DCS in Figures 21 and 23. The maximum frequency for $1\lambda \times 1\lambda$ resistive plate is 1 for the bistatic case. Since the sampling frequency must be twice the maximum frequency component of the signal, the sampling frequency is 2, which corresponds to $0.5\lambda \times 0.5\lambda$ patch size. Applying this procedure to a $3\lambda \times 3\lambda$ plate yielded the same maximum patch size. The required sampling frequency approaches zero as the plate size gets smaller, as expected. Thus in the case of bistatic RCS synthesis a half-wavelength subdomain size corresponds to the Nyquist sampling rate. Note that this guideline applies only to cases where the RCS pattern is highly periodic (i.e., negligible multiple reflections, surface waves, diffraction, etc.). When these other scattering mechanisms are present the scattering pattern becomes more complicated and thus contains more high-frequency components. Also, it is important to note that satisfying the field

sampling rate does not insure that the series expansion for the current on the plate is converged.
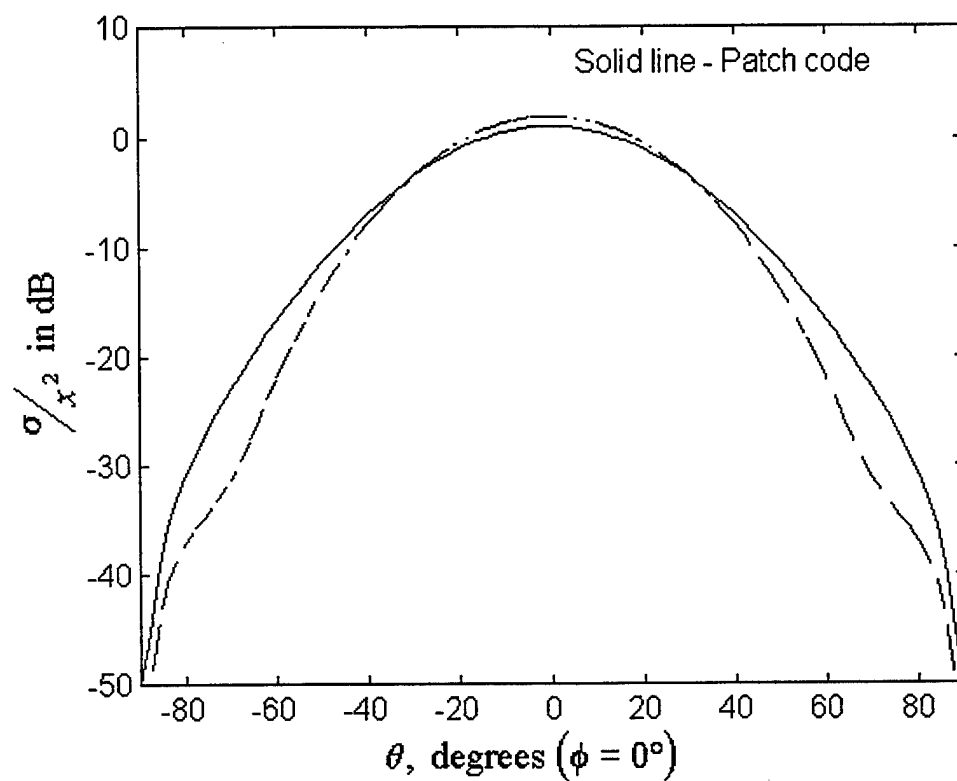

Figure 6. Comparison of the bistatic RCS computed with PATCH vs that with rectangular patches ($R_S = 377$, $N_x = N_y = 8$, $L_x = L_y = 1\lambda$ and $\theta_i = \phi_i = 0°$).
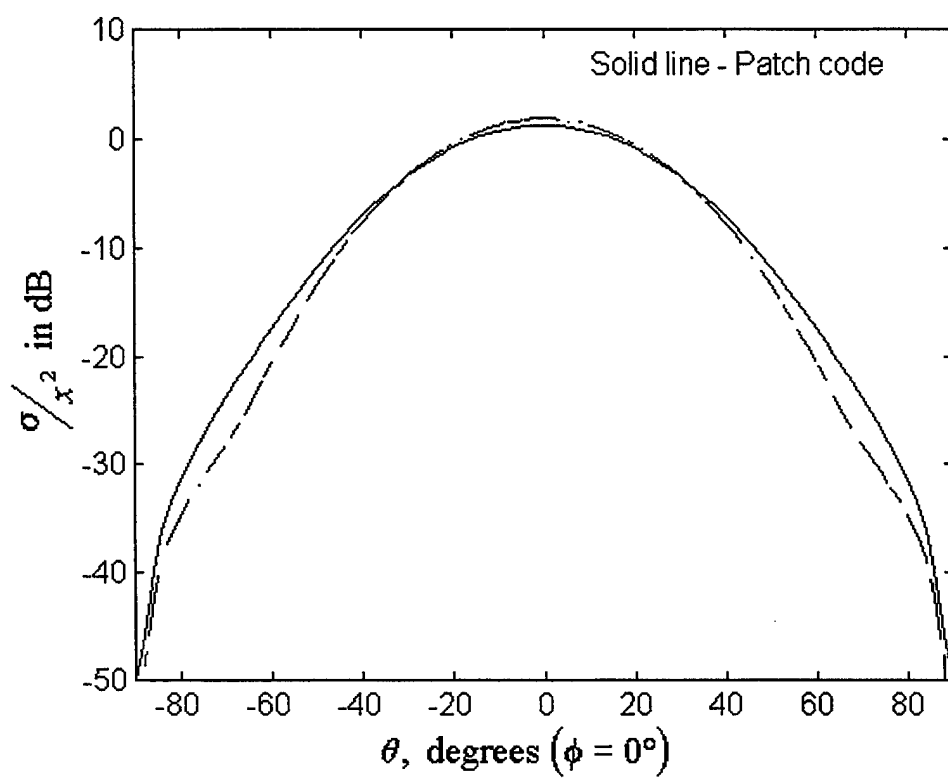
Figure 7. Comparison of the bistatic RCS computed with PATCH vs that with rectangular patches ($R_S = 377$, $N_x = N_y = 14$, $L_x = L_y = 1\lambda$ and $\theta_i = \phi_i = 0°$).

29

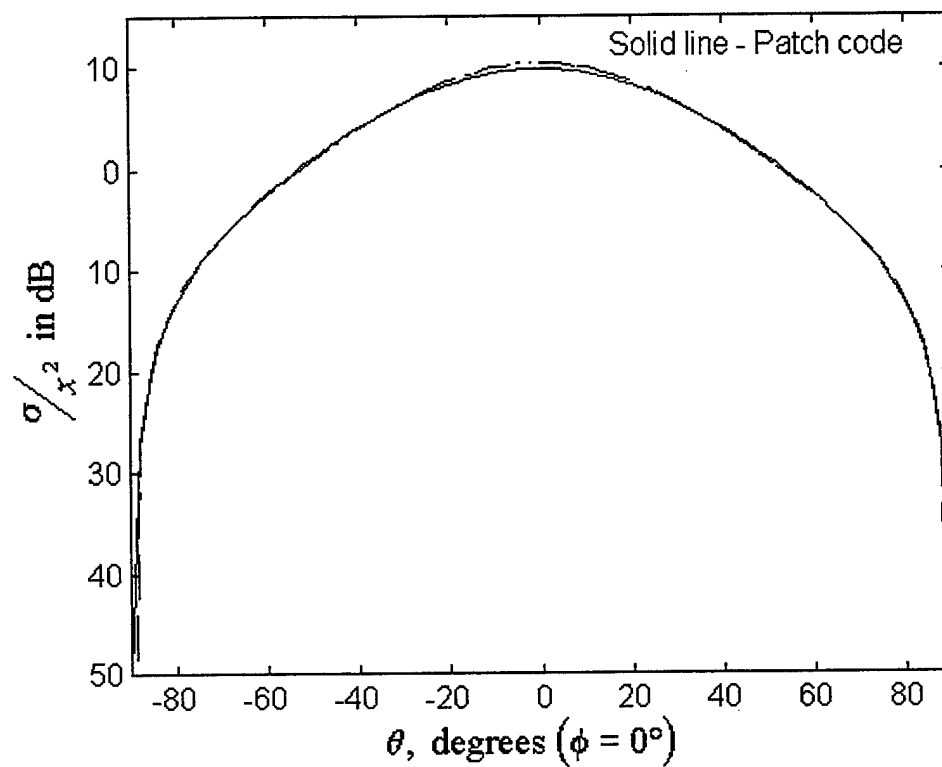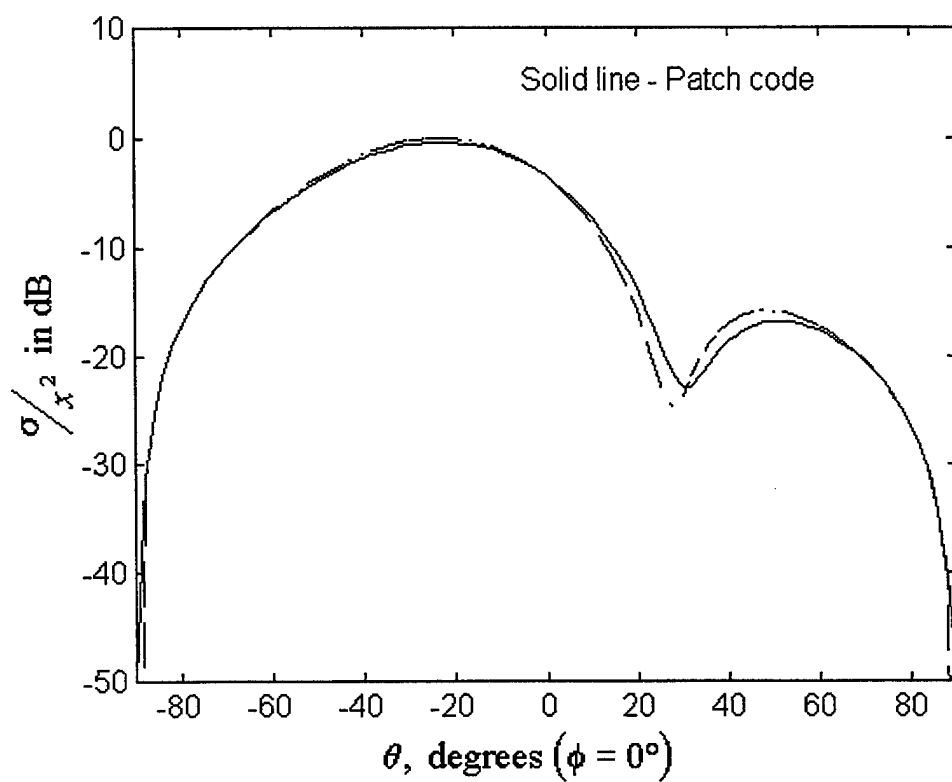Figure 8.   Comparison of the bistatic RCS computed with PATCH vs that with rectangular patches ($R_S = 10$, $N_x = N_y = 20$, $L_x = L_y = 1\lambda$ and $\theta_i = \phi_i = 0°$).

Figure 9.   Comparison of the bistatic RCS computed with PATCH vs that with rectangular
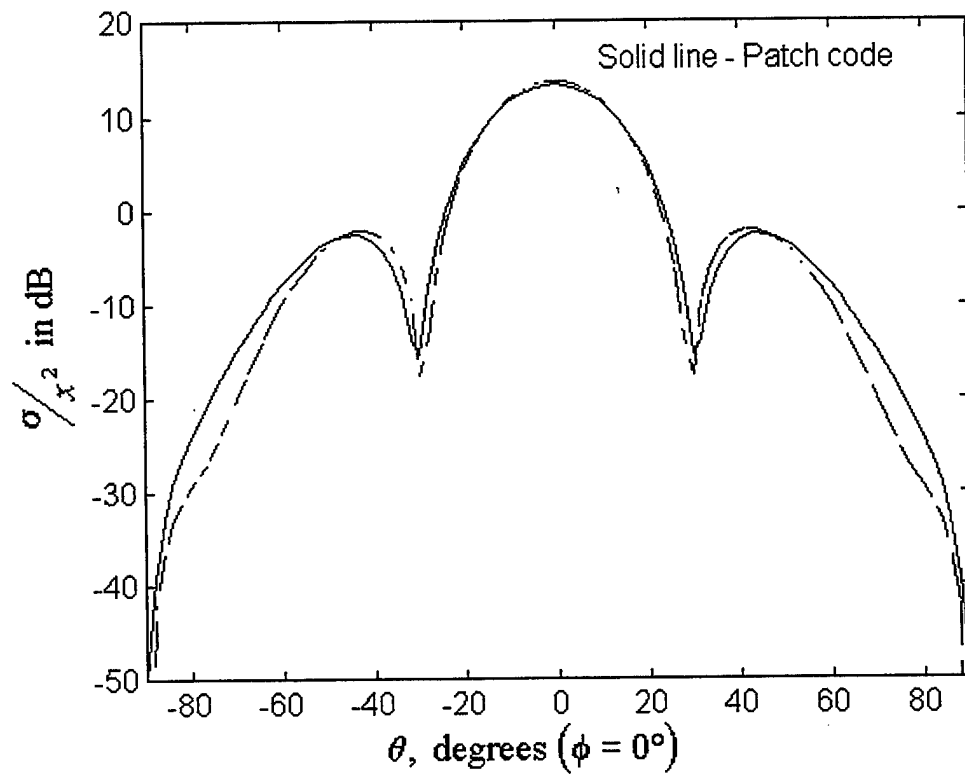patches ($R_S = 377$, $N_x = N_y = 20$, $L_x = L_y = 1\lambda$ and $\theta_i = 30°$, $\phi_i = 0°$).

Figure 10. Comparison of the bistatic RCS computed with PATCH vs that with rectangular patches ($R_S = 377$, $N_x = N_y = 20$, $L_x = L_y = 2\lambda$ and $\theta_i = \phi_i = 0°$).
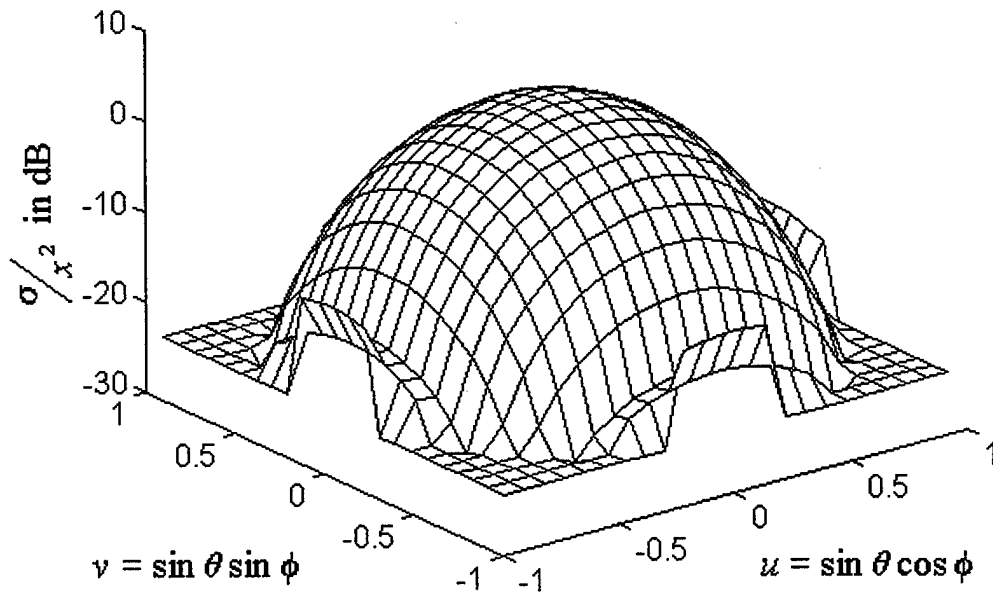
32

Figure 11. Two dimensional plot of the bistatic RCS of a rectangular resistive sheet ($R_s = 377$, $N_u = N_v = 23$, ($N_x = N_v$, $N_y = N_v$), $L_x = L_y = 1\lambda$ and $\theta_i = \phi_i = 0°$).
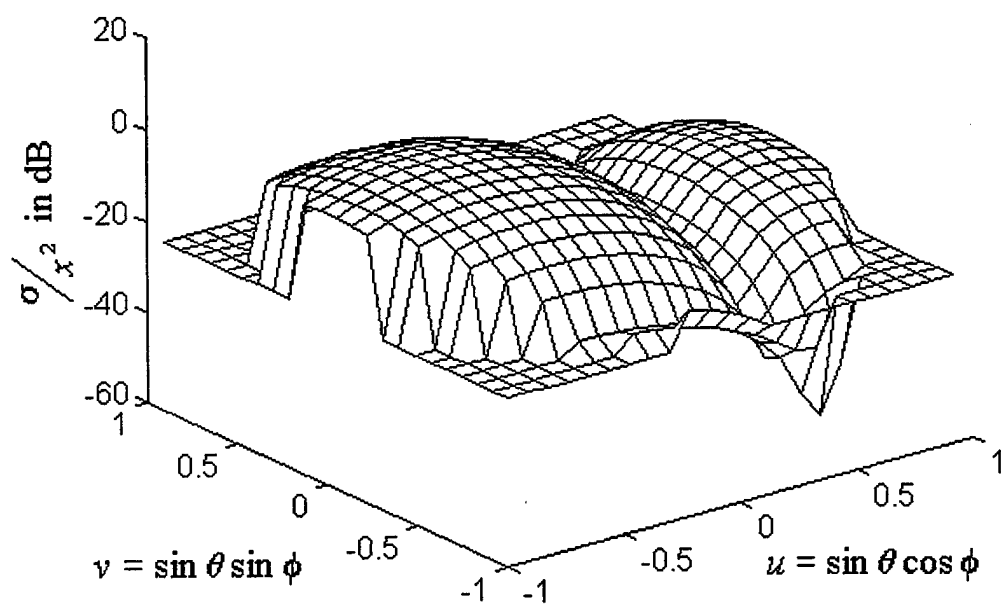
Figure 12. Two dimensional plot of the bistatic RCS of a rectangular resistive sheet ($R_S =$ 377, $L_x = L_y = 1\lambda$ and $\theta_i = 30°$, $\phi_i = 0°$).

Figure 13. Residual resistivity for $R_{so} = 377$, $N_u = N_v = 4$ ($N_x = N_u$, $N_y = N_v$), $L_x = L_y = 1\lambda$ and normal incidence.

Figure 14. Residual resistivity for $R_{so} = 10$, $N_u = N_v = 9$ ($N_x = N_u$, $N_y = N_v$), $L_x = L_y = 1\lambda$ and normal incidence.

Figure 15. Residual resistivity for R_{so} = 377, N_u = N_v = 16 (N_x = N_u, N_y = N_v), L_x = L_y = 1λ and normal incidence.

Figure 16. Residual resistivity for $R_{so} = 377$, $N_u = N_v = 16$ ($N_x = N_u$, $N_y = N_v$), $L_x = L_y = 1\lambda$ and $\theta_i = 30°$, $\phi_i = 0°$.
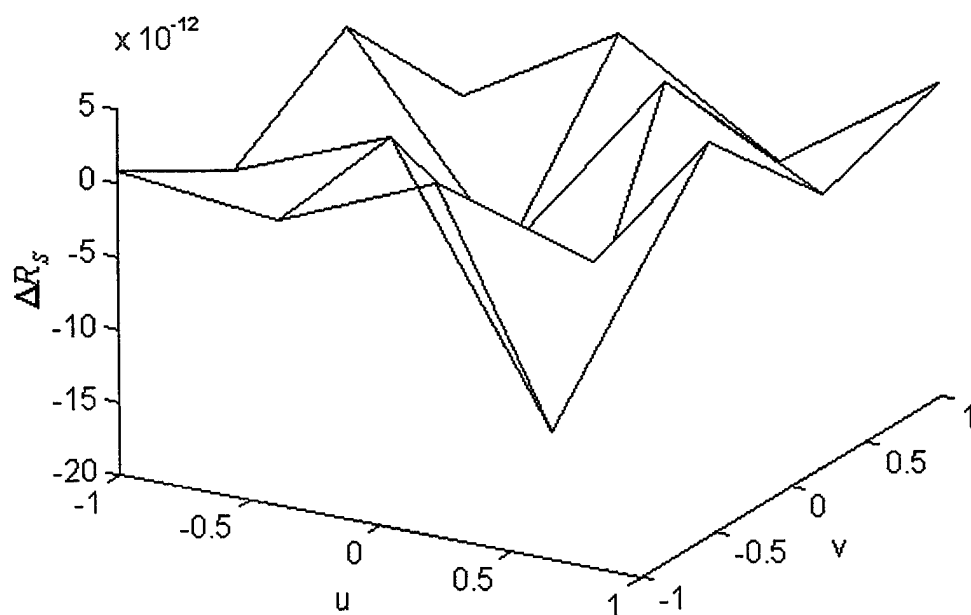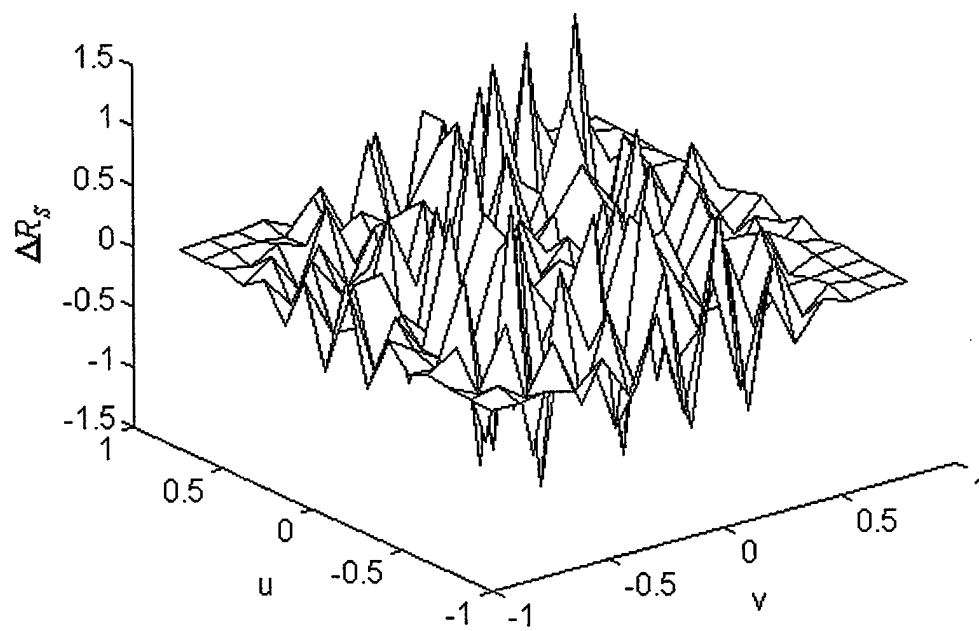
Figure 17. Residual resistivity for $R_{so} = 377$, $N_u = N_v = 16$ ($N_x = N_u$, $N_y = N_v$), $L_x = L_y = 2\lambda$ and normal incidence.
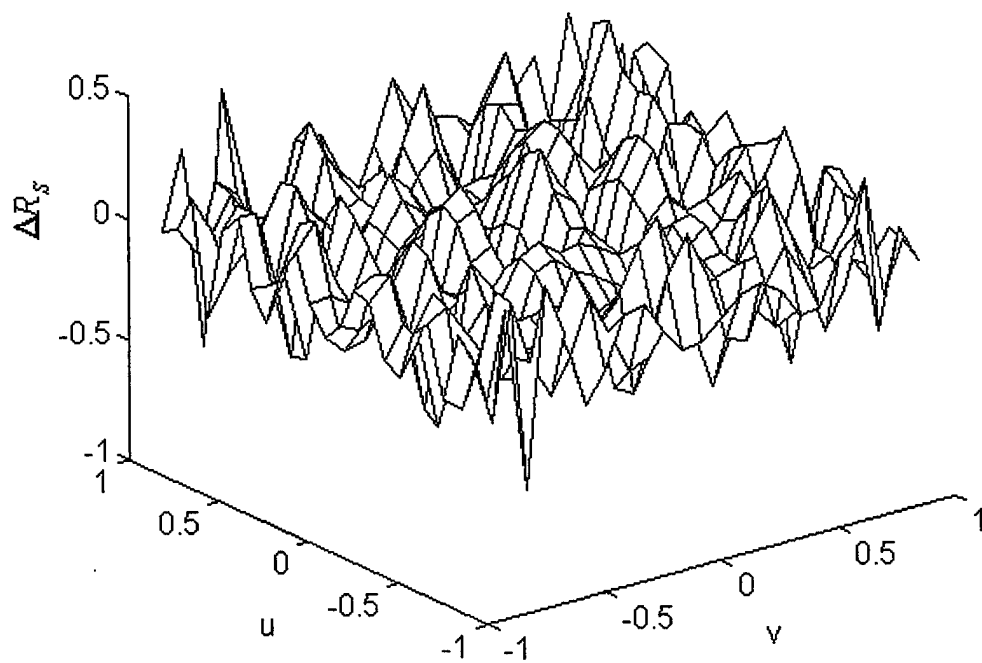
Figure 18. Residual resistivity for $R_{so} = 377$, $N_u = N_v = 23$ ($N_x = N_u$, $N_y = N_v$), $L_x = L_y = 1\lambda$ and normal incidence.

40
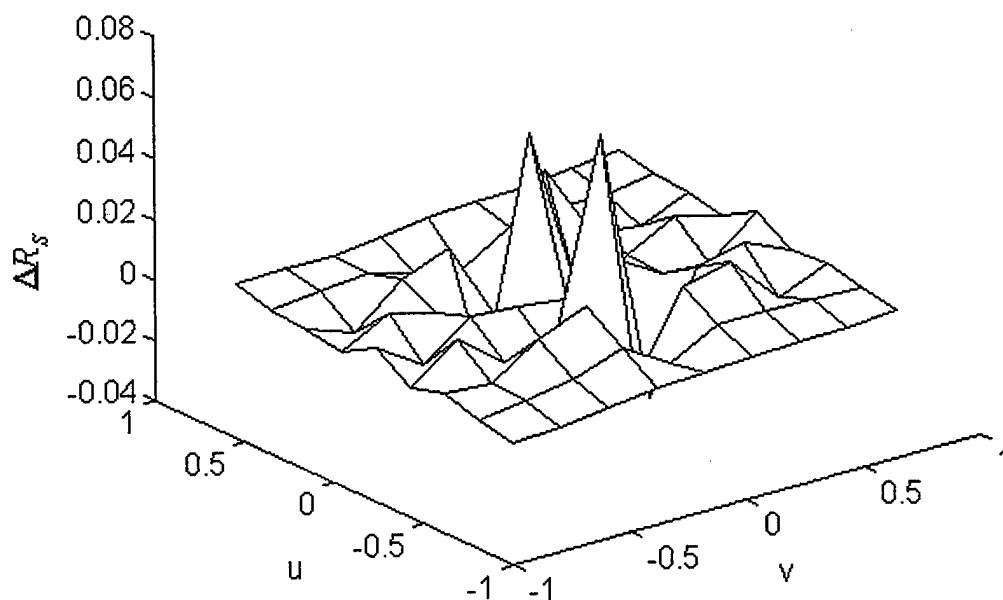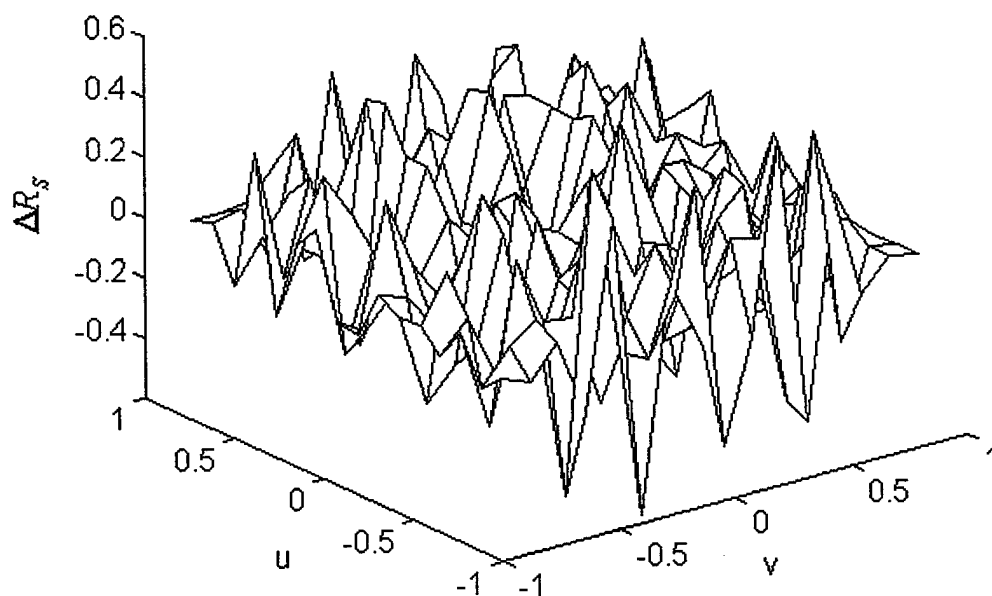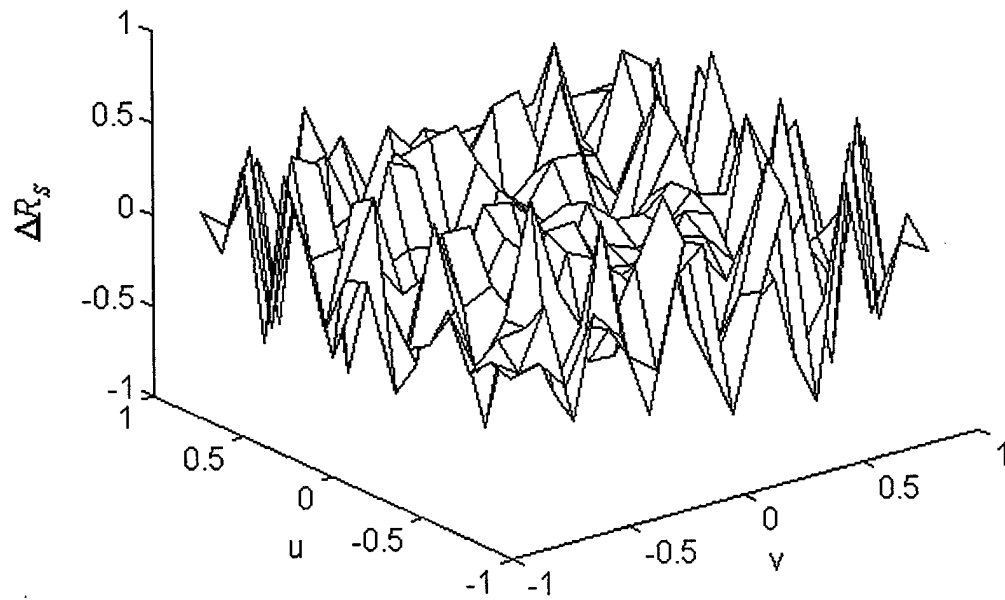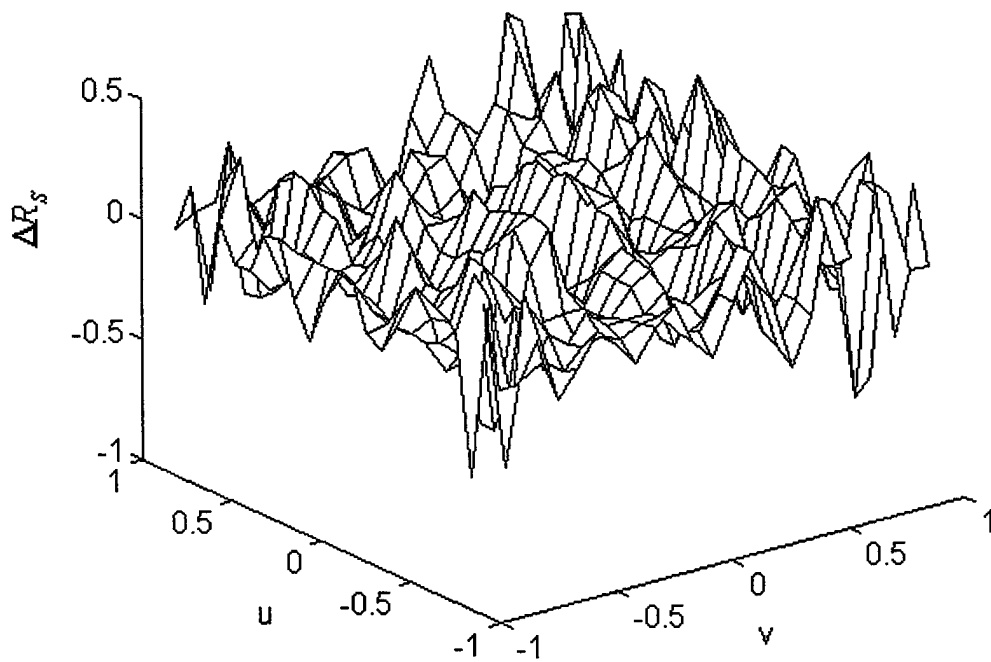
Figure 19. Residual resistivity for $R_{so} = 377$, $N_u = N_v = 23$ ($N_x = N_u$, $N_y = N_v$), $L_x = L_y = 1\lambda$ and $\theta_i = 30°$, $\phi_i = 0°$.
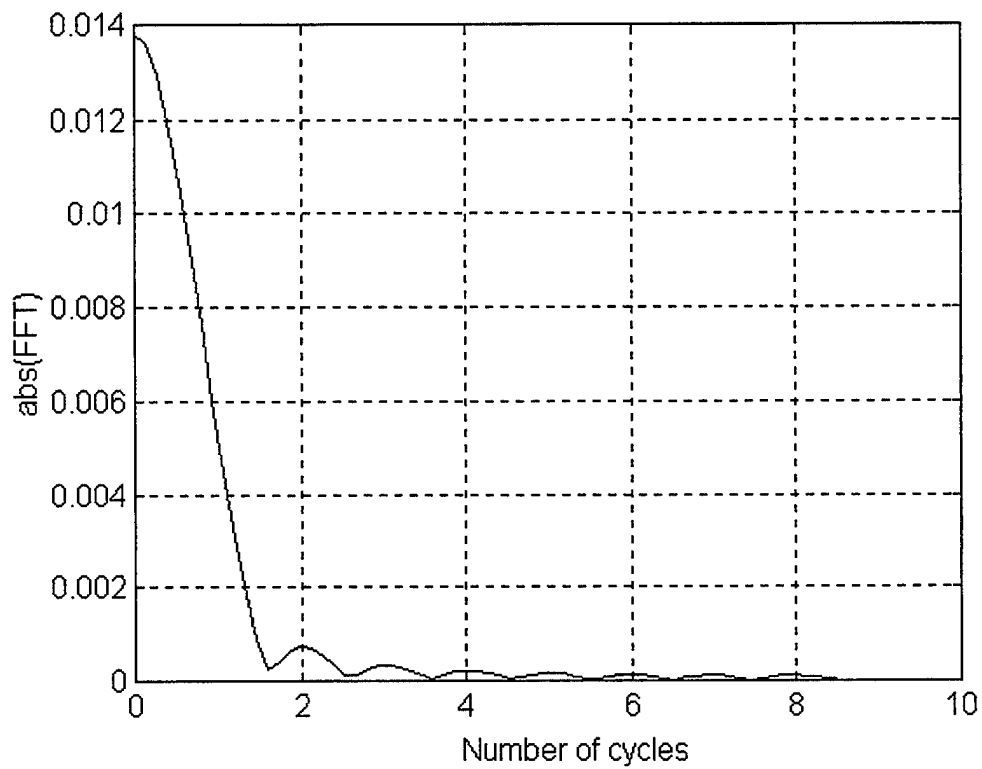
Figure 20. Frequency analysis of one row (or u coordinate) of the scattered E-field. Maximum frequency is 1 for $R_{so} = 377$, $L_x = L_y = 1\lambda$, 256 field points and normal incidence.
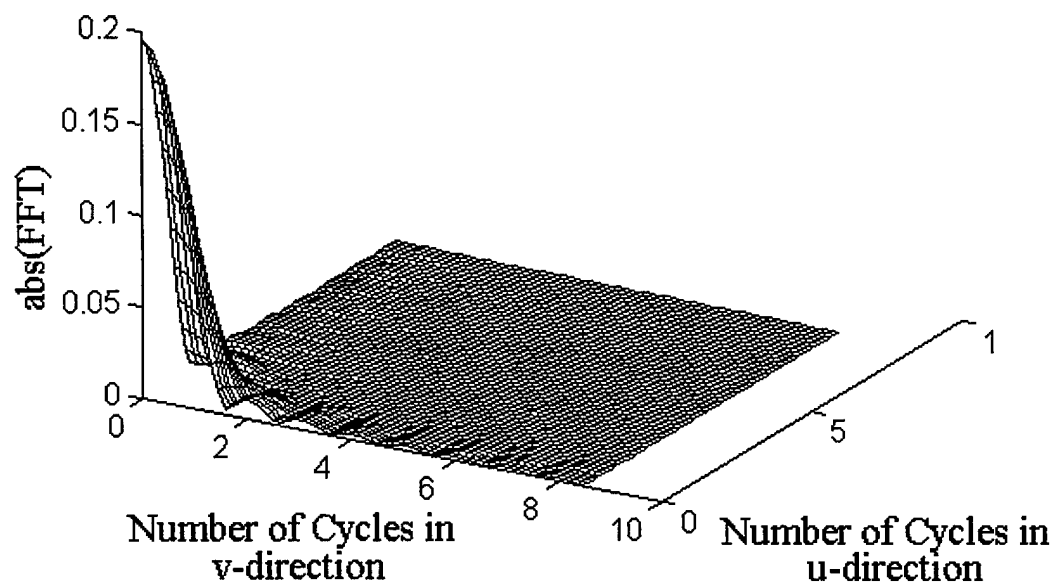
Figure 21. Frequency analysis in two-dimensions for the scattered E-field. Maximum frequency is 1 for $R_{so} = 377$, $L_x = L_y = 1\lambda$, 256 field points and normal incidence.
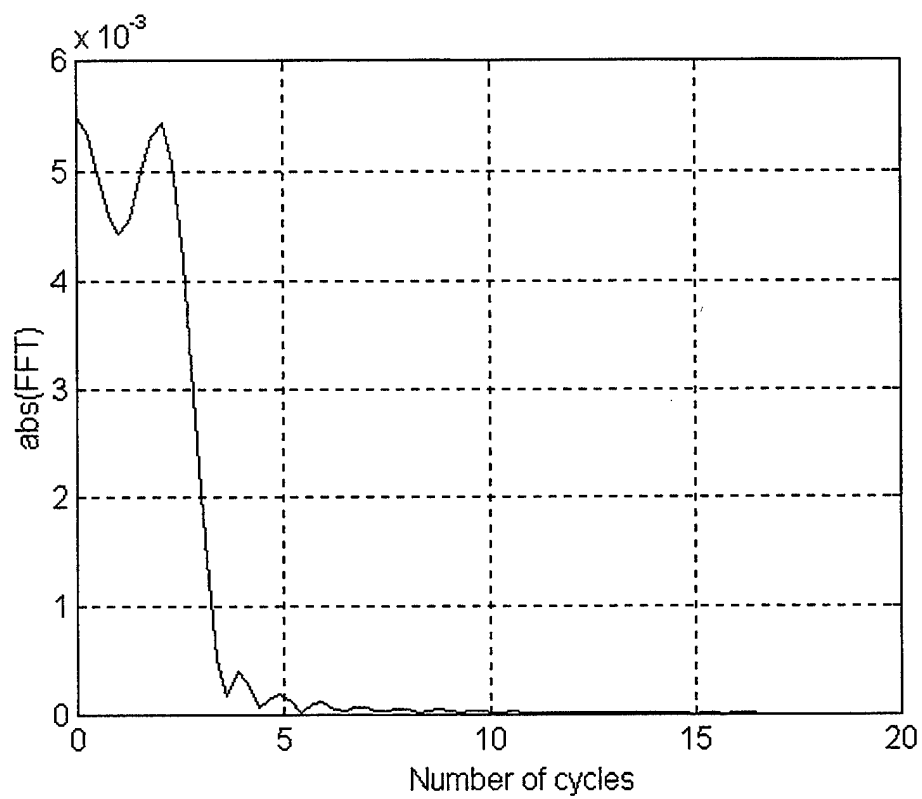
Figure 22. Frequency analysis of one row (or one column) of the scattered E-field. Maximum frequency is 3 for $R_{so}= 377$, $L_x= L_y= 3\lambda$, 900 field points and normal incidence.
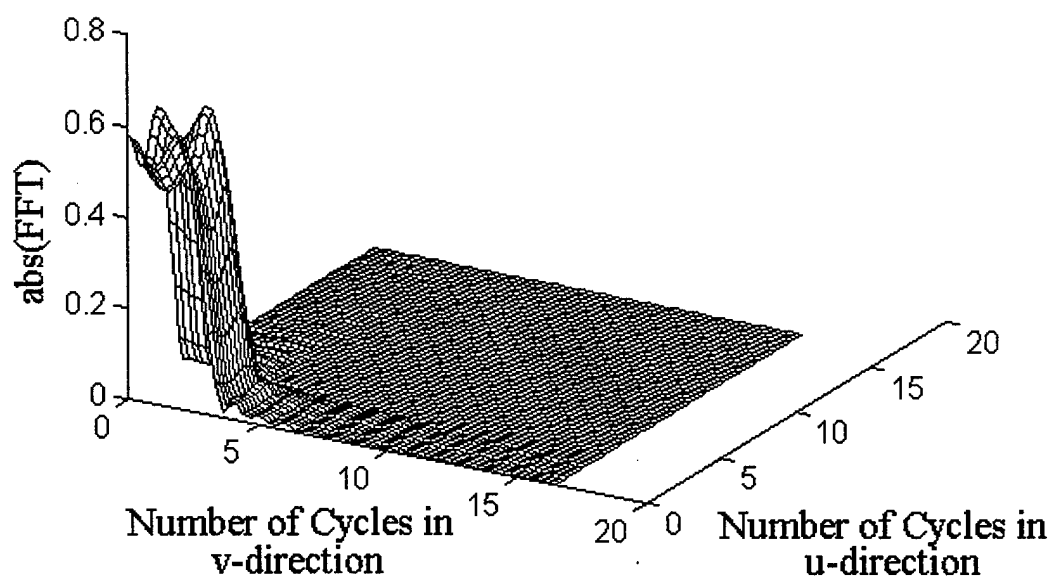
Figure 23. Frequency analysis in two-dimension for the scattered E-field. Maximum frequency is 3 for $R_{so} = 377$, $L_x = L_y = 3\lambda$, 900 field points and normal incidence.

45

V. CONCLUSIONS

A rigorous bistatic RCS synthesis method for flat rectangular sheets has been presented. For convenience, the research was limited to resistive surfaces and parallel polarization. The scattering and synthesis equations are based on the method of moments (MM) technique. A rigorous method requires that both the current and resistivity be expanded into series, and the unknown coefficients determined simultaneously.

The scattered field for a resistive sheet was first calculated for a known resistivity. The bistatic RCS of the resistive sheet was used to validate the rectangular patch solution by comparing it with the output of PATCH for different cases. This direct problem solution was used to generate and validate the synthesis procedure. The unknown current and resistivity coefficients were found by solving two coupled integral equations (equations (15) and (16)). The reconstructed and original resistivities were compared to verify the synthesis equations. A parametric study of the solution convergence was performed. In all cases, the reconstructed resistivity obtained from the synthesis equations was in agreement with the original resistivity.

The frequency content of the scattered electric field was also investigated in order to determine the maximum allowable patch size. The number of far-field points must be equal to the number of patches on the plate to obtain a unique solution. If the field pattern is highly periodic in DCS, as in the case of the physical optics solution, the Nyquist sampling theorem yields approximately 0.5λ patch size on the plate for bistatic RCS. However, a MM solution with 0.5λ patches is usually not converged; the conventional guideline is 0.1λ subdomains. However, in many cases of practical interest where the patterns to be synthesized are primarily determined by specular scattering (i.e., negligible surface waves and multiple reflection and diffraction) the minimum patch size can possibly be larger than the usual 0.1λ.

The rigorous solution presented in this thesis is limited to flat rectangular resistive sheets. This allowed the use of rectangular subdomains with pulse basis functions. Pulse

47

basis functions are convenient for computer programming and result in matrix synthesis equations that are easy to solve. However, the more important scattering problems involve doubly curved surfaces. For these targets triangular subdomains must be used to accurately represent the surface. The overlapping basis functions of the type used in PATCH will result in much more complicated (and possibly nonlinear) sets of equations. It is recommended that this be the direction of future research in this area.

APPENDIX COMPUTER CODES

In this appendix computer codes are presented. The code *plate.m* calculates the RCS in θ-direction for the bistatic case and TM_z polarization. The code *platedcs.m* calculates the RCS and plots it in direction cosine space. The data from this code is saved to be used in the synthesis program. The code *synt.m* uses the stored data to reconstruct the surface resistivity. The codes *dcsin.m, center.m, green.m, green1.m, green2.m, green3.m,* and *green4.m* are the functions which are used in the synthesis and scattering programs. The code *sample.m* performs the FFT analysis in the u and v directions of the scattered field. Detailed explanations are presented in the comments in the codes.

```
%%%%%%%%%%%%%%%%%%%%%%%%%%%%%%%%%%%%%%%%%%%%%%%%%%
%                    plate.m                     %
% Resistive Square Plate Bistatic RCS (in teta direction)  %
% with Method of Moments.                        %
%                                                %
% Ugurcan Samli,  July 1996                      %
%                                                %
%%%%%%%%%%%%%%%%%%%%%%%%%%%%%%%%%%%%%%%%%%%%%%%%%%

clear all;
format compact;

%%%%%%%%%%%%%%% Variables used in the program%%%%%%%%%%%%%%%

% modex and modey are the number of patches in x- and y-directions
% respectively. Eotet and Eophi are for polarization. Rs is the
% constant surface resistivity.

Lx=1;              % input('Length in x-direction= ');
Ly=1;              % input('Length in y-direction= ');
modex=20; modey=20;
deltax=Lx/modex; deltay=Ly/modey;
mode=modex*modey; eta=377; lambda=1;
k=2*pi; t=pi/180; Rreal=377; Rimg=0;
Eotet=1; Eophi=0; Emag=sqrt(Eotet^2+Eophi^2);
incr=2; sta=-90; stp=90;
lim=floor((stp-sta+1e-5)/incr)+1;
int=2; phiang=0; phi=phiang*t;

Rs1=Rreal+j*Rimg; Rs2=Rs1*eye(mode); Rs=diag(Rs2)';

%%%%%%%%%% Computing patch center points %%%%%%%

in=0;
for s=1:modey
 for ss=1:modex
  in=in+1;

  xn(in)=(-Lx/2+deltax/2+(ss-1)*deltax);
  yn(in)=(-Ly/2+deltay/2+(s-1)*deltay);

 end;
```

50

```
end;

xm=xn;  ym=yn;

fun1=j*k*eta; fun2=j/k*eta;

%%%%%%%%% Calculation of impedance matrix %%%%%%%%%%%%%

% Impedance matrix calculation is same with the impedance matrix
% calculation in platedcs.m, green functions are used in calculations.

for n=1:mode
 for m=1:mode

 Gxx=green(xm(m),xn(n),ym(m),yn(n),deltax,deltay,int);
 Gyy=green(ym(m),yn(n),xm(m),xn(n),deltay,deltax,int);

 xn1=xn(n)+deltax/2;
 xn2=xn(n)-deltax/2;
 xm1=xm(m)+deltax/2;
 xm2=xm(m)-deltax/2;
 yn1=yn(n)+deltay/2;
 yn2=yn(n)-deltay/2;
 ym1=ym(m)+deltay/2;
 ym2=ym(m)-deltay/2;

 Qxx=(green1(xm2,xn2,ym(m),yn(n),deltax,deltay,int)...
        -green1(xm2,xn1,ym(m),yn(n),deltax,deltay,int)...
        -green1(xm1,xn2,ym(m),yn(n),deltax,deltay,int)...
        +green1(xm1,xn1,ym(m),yn(n),deltax,deltay,int));
 Qxy=(green2(xm2,xn(n),ym(m),yn2,deltax,deltay,int)...
        -green2(xm2,xn(n),ym(m),yn1,deltax,deltay,int)...
        -green2(xm1,xn(n),ym(m),yn2,deltax,deltay,int)...
        +green2(xm1,xn(n),ym(m),yn1,deltax,deltay,int));
 Qyx=(green3(xm(m),xn2,ym2,yn(n),deltax,deltay,int)...
        -green3(xm(m),xn2,ym1,yn(n),deltax,deltay,int)...
        -green3(xm(m),xn1,ym2,yn(n),deltax,deltay,int)...
        +green3(xm(m),xn1,ym1,yn(n),deltax,deltay,int));
 Qyy=(green4(xm(m),xn(n),ym2,yn2,deltax,deltay,int)...
        -green4(xm(m),xn(n),ym2,yn1,deltax,deltay,int)...
        -green4(xm(m),xn(n),ym1,yn2,deltax,deltay,int)...
        +green4(xm(m),xn(n),ym1,yn1,deltax,deltay,int));
```

51

```
sum=fun1*Gxx-fun2*Qxx;
 if m==n, sum=sum+Rs(m)*(deltax/deltay); end
Z(m,n)=sum;

sum=-fun2*Qxy;
Z(m,n+mode)=sum;

sum=-fun2*Qyx;
Z(m+mode,n)=sum;

sum=fun1*Gyy-fun2*Qyy;
 if m+mode==n+mode, sum=sum+Rs(m)*(deltay/deltax); end
Z(m+mode,n+mode)=sum;

end;
end;

ZI=pinv(Z);
disp('Impedence Matrix Computed and Inverted');

%%%%%%%%%%%%%% Incidence angle %%%%%%%%%%%%%%

phii=0; teti=0;
sinphii=sin(phii*t); sinteti=sin(teti*t);
cosphii=cos(phii*t); costeti=cos(teti*t);

vvi=sinphii*sinteti;
uui=sinteti*cosphii;

Ex=Eotet*costeti*cosphii-Eophi*sinphii;
Ey=Eotet*costeti*sinphii+Eophi*cosphii;

 for n=1:mode;
  argx=k*deltax*uui/2;
  argy=k*deltay*vvi/2;
  sincx=1; sincy=1;
  if abs(argx)>1e-5, sincx=sin(argx)/argx; end
  if abs(argy)>1e-5, sincy=sin(argy)/argy; end
  expxy=exp(j*k*(xn(n)*uui+yn(n)*vvi));
  vx(n)=Ex*deltax*expxy*sincx*sincy;
  vy(n)=Ey*deltay*expxy*sincx*sincy;
```

```
end;

% Excitation vector V, and current coefficients I.

V(1:mode)=vx(:);
V(mode+1:2*mode)=vy(:);
I=ZI*V.';

%%%%%%%% calculation of the scattered fields %%%%%%%%%%

 for aa=1:lim;
  angle(aa)=(aa-1)*incr+sta;
  teta=angle(aa)*t;
  costet=cos(teta);
  sintet=sin(teta);
  cosphi=cos(phi);
  sinphi=sin(phi);
  vv=sinphi*sintet;
  uu=sintet*cosphi;

  for n=1:mode
   argx=k*deltax*uu/2;
   argy=k*deltay*vv/2;
   sincx=1; sincy=1;
   if abs(argx)>1e-5, sincx=sin(argx)/argx; end
   if abs(argy)>1e-5, sincy=sin(argy)/argy; end
   expxy=exp(j*k*(xn(n)*uu+yn(n)*vv));
   vx1(n)=deltax*expxy*sincx*sincy;
   vy1(n)=deltay*expxy*sincx*sincy;
  end;

  Exs=vx1*I(1:mode);
  Eys=vy1*I(mode+1:2*mode);

%%%% TM and TE polarization cases are together.%%%%%

  etet=-j*k*eta/2/k*(Exs*costet*cosphi+Eys*costet*sinphi);
  ephi=-j*k*eta/2/k*(-Exs*sinphi+Eys*cosphi);
  etetrcs(aa)=etet;
  ephircs(aa)=ephi;

 end;
```

%%%%%%% Calculation of the RCS, and plots %%%%%%%

```
RCStet=10*log10(abs(etetrcs).^2*2*k+1e-10);
RCSphi=10*log10(abs(ephircs).^2*2*k+1e-10);

plot(angle,RCStet),grid;
max1=max(max(RCStet));
db=(floor(max(max1)/5)+1)*5;
axis([-90,90,db-50,db]);
xlabel('Angle in degrees');
ylabel('RCS in dBsm ');
title('Bistatic RCS of a Resistive Plate With MM');

%save f1 Z RCStet angle Rreal
```

```
%%%%%%%%%%%%%%%%%%%%%%%%%%%%%%%%%%%%%%%%%%%%%%%%%%%
%                       platedcs.m                              %
%  This program calculates Resistive Square Plate Bistatic RCS with  %
%  Moment Method, and it plots this RCS in direction cosine space.   %
%                                                                %
%  Ugurcan Samli.                                                %
%                                                                %
%%%%%%%%%%%%%%%%%%%%%%%%%%%%%%%%%%%%%%%%%%%%%%%%%%%

clear all;
format compact;

%%%%%%%%%%%%% Variables used in the program %%%%%%%%%%%%%

Lx=1;          % input('Length in x-direction= ');
Ly=1;          % input('Length in y-direction= ');
T=1;           % If the number of field points equal to number of
               % patches, T=1.
% modex and modey are the number of segments in x and y direction.
% Eotet and Eophi determines the polarization (Eotet=1 and Eophi=0
% is the Teta polarization.)
eta=377; lambda=1; k=2*pi; t=pi/180; int=2;
Rreal=377; Rimg=0;
Eotet=1; Eophi=0;

% Finding center of the patches in Direction Cosine Space.
% dcsin.m and center.m functions are called.
modex=4; modey=3;
deltax=Lx/modex; deltay=Ly/modey;
mode=modex*modey;
load uv1          % u and v points are computed seperately.

% Constant surface resistivity Rs matrix.
Rs1=Rreal+j*Rimg; Rs2=Rs1*eye(mode); Rs=diag(Rs2)';

%%%%%%%%%%% Computing Patch center points. %%%%%%%%%%%%%%

in=0;
for s=1:modey
 for ss=1:modex
  in=in+1;
  xn(in)=(-Lx/2+deltax/2+(ss-1)*deltax);
```

```
    yn(in)=(-Ly/2+deltay/2+(s-1)*deltay);
  end;
end;

xm=xn; ym=yn;

fun1=j*k*eta; fun2=j/k*eta;

%%%%%%% Filling Impedence Matrix %%%%%%%%%%%%%%

% Green functions are called in the impedance matrix calculation.
for n=1:mode
  for m=1:mode

        Gxx=green(xm(m),xn(n),ym(m),yn(n),deltax,deltay,int);
        Gyy=green(ym(m),yn(n),xm(m),xn(n),deltay,deltax,int);

        xn1=xn(n)+deltax/2;
        xn2=xn(n)-deltax/2;
        xm1=xm(m)+deltax/2;
        xm2=xm(m)-deltax/2;
        yn1=yn(n)+deltay/2;
        yn2=yn(n)-deltay/2;
        ym1=ym(m)+deltay/2;
        ym2=ym(m)-deltay/2;

        Qxx=(green1(xm2,xn2,ym(m),yn(n),deltax,deltay,int)...
           -green1(xm2,xn1,ym(m),yn(n),deltax,deltay,int)...
           -green1(xm1,xn2,ym(m),yn(n),deltax,deltay,int)...
           +green1(xm1,xn1,ym(m),yn(n),deltax,deltay,int));
        Qxy=(green2(xm2,xn(n),ym(m),yn2,deltax,deltay,int)...
           -green2(xm2,xn(n),ym(m),yn1,deltax,deltay,int)...
           -green2(xm1,xn(n),ym(m),yn2,deltax,deltay,int)...
           +green2(xm1,xn(n),ym(m),yn1,deltax,deltay,int));
        Qyx=(green3(xm(m),xn2,ym2,yn(n),deltax,deltay,int)...
           -green3(xm(m),xn2,ym1,yn(n),deltax,deltay,int)...
           -green3(xm(m),xn1,ym2,yn(n),deltax,deltay,int)...
           +green3(xm(m),xn1,ym1,yn(n),deltax,deltay,int));
        Qyy=(green4(xm(m),xn(n),ym2,yn2,deltax,deltay,int)...
           -green4(xm(m),xn(n),ym2,yn1,deltax,deltay,int)...
           -green4(xm(m),xn(n),ym1,yn2,deltax,deltay,int)...
           +green4(xm(m),xn(n),ym1,yn1,deltax,deltay,int));
```

```
            sum=fun1*Gxx-fun2*Qxx;
             if m==n, sum=sum+Rs(m)*(deltax/deltay); end
            Z(m,n)=sum;

            sum=-fun2*Qxy;
            Z(m,n+mode)=sum;

            sum=-fun2*Qyx;
            Z(m+mode,n)=sum;

            sum=fun1*Gyy-fun2*Qyy;
             if m+mode==n+mode, sum=sum+Rs(m)*(deltay/deltax); end
            Z(m+mode,n+mode)=sum;

        end;
    end;

ZI=inv(Z);
disp('Impedence Matrix Computed and Inverted');

%%%%%%% Incident Angles %%%%%%%%%%

phii=0; teti=0;
sinphii=sin(phii*t); sinteti=sin(teti*t);
cosphii=cos(phii*t); costeti=cos(teti*t);

vvi=sinphii*sinteti;
uui=sinteti*cosphii;

Ex=Eotet*costeti*cosphii-Eophi*sinphii;
Ey=Eotet*costeti*sinphii+Eophi*cosphii;

 for n=1:mode;
   argx=k*deltax*uui/2;
   argy=k*deltay*vvi/2;
   sincx=1; sincy=1;
   if abs(argx)>1e-5, sincx=sin(argx)/argx; end;
   if abs(argy)>1e-5, sincy=sin(argy)/argy; end;
   expxy=exp(j*k*(xn(n)*uui+yn(n)*vvi));
   vx(n)=Ex*deltax*expxy*sincx*sincy;
   vy(n)=Ey*deltay*expxy*sincx*sincy;
```

```
end;

% Excitation vector and current coefficients, V and I respectively.
V(1:mode)=vx(:);
V(mode+1:2*mode)=vy(:);
I=ZI*V.';

%%%%%%%%% calculation of the field points%%%%%%%%%

for m=1:mode
 unit1(m)=(sqrt(u(m)^2+v(m)^2));
 phi(m)=(atan2(u(m)+1e-7,v(m)));
 teta(m)=asin(unit1(m));
 costet=cos((teta(m)));
 sintet=sin((teta(m)));
 cosphi=cos(phi(m));
 sinphi=sin(phi(m));

  for n=1:mode
   argx=k*deltax*u(m)/2;
   argy=k*deltay*v(m)/2;
   sincx=1; sincy=1;
   if abs(argx)>1e-5, sincx=sin(argx)/argx; end
   if abs(argy)>1e-5, sincy=sin(argy)/argy; end
   expxy=exp(j*k*(xn(n)*u(m)+yn(n)*v(m)));
   vx1(n)=deltax*expxy*sincx*sincy;
   vy1(n)=deltay*expxy*sincx*sincy;
  end;

% x- and y-components of the scattered field.
  Exs=vx1*I(1:mode); Exs1(m)=Exs;
  Eys=vy1*I(mode+1:2*mode); Eys1(m)=Eys;

  etet=-j*k*eta/2/k*(Exs*costet*cosphi+Eys*costet*sinphi); etet1(m)=etet;
  ephi=-j*k*eta/2/k*(-Exs*sinphi+Eys*cosphi); ephi1(m)=ephi;

  etetrcs(m)=(-j*k*eta/2/k)*Exs;
  ephircs(m)=(-j*k*eta/2/k)*(Eys);

end;

%%%%%%%%% Calculation of RCS %%%%%%%%%%
```

```
for i=1:mode
 RCStet(i)=10*log10(abs(etetrcs(i)).^2*2*k+1e-10);
 RCSphi(i)=10*log10(abs(ephircs(i)).^2*2*k+1e-10);
end;

RCS=reshape(RCStet,modex,modey);

u=reshape(u,modex,modey); v=reshape(v,modex,modey);

mesh(u,v,RCS);

% All the  data are saved for use in synthesis program.
save b24 RCS u v mode modex modey Exs1 Eys1 V Z deltax deltay xn xm yn ym Rs I
etetrcs ephircs etet1 ephi1 etet ephi phii teti RCSphi
```

```
%%%%%%%%%%%%%%%%%%%%%%%%%%%%%%%%%%%%%%%%%%%%%%%
%                       synt.m                          %
%                                                       %
%  This program calculates the synthesis results for bistatic case.  %
%  The result will be the resistivity which is found    %
%  from the synthesis equations.                        %
%                                                       %
%  Ugurcan Samli, July 1996                             %
%                                                       %
%%%%%%%%%%%%%%%%%%%%%%%%%%%%%%%%%%%%%%%%%%%%%%%


clear all;
format long;

% Reading in the data file from the scatterring program (platedcs.m)

load b24.mat;
disp('Data file is loaded.');

eta=377; lambda=1; t=pi/180; k=2*pi;
uxx=linspace(-1,1,mode);
vyy=linspace(-1,1,mode);

% Reading the E-field components from the data file.

efld(1:mode)=Exs1(:); efld(mode+1:2*mode)=Eys1(:);
rs=[Rs,Rs]; rs=diag(rs);

%%%%%%%%%% Filling the matrices %%%%%%%%%%%%%%%

% Original resistivity is subtracted from the impedance matix.

Z=Z-rs;

for m=1:mode

   for n=1:mode

   argy=k*deltay*v(m)/2;
   argx=k*deltax*u(m)/2;
   sincx=1; sincy=1;
```

60

```
%%%%%%%%%%%%%%%%%%%%%%%%%%%%%%%%%%%%%%%%%%%%%%%
%                       synt.m                          %
%                                                       %
%  This program calculates the synthesis results for bistatic case.  %
%  The result will be the resistivity which is found    %
%  from the synthesis equations.                        %
%                                                       %
%  Ugurcan Samli, July 1996                             %
%                                                       %
%%%%%%%%%%%%%%%%%%%%%%%%%%%%%%%%%%%%%%%%%%%%%%%


clear all;
format long;

% Reading in the data file from the scatterring program (platedcs.m)

load b24.mat;
disp('Data file is loaded.');

eta=377; lambda=1; t=pi/180; k=2*pi;
uxx=linspace(-1,1,mode);
vyy=linspace(-1,1,mode);

% Reading the E-field components from the data file.

efld(1:mode)=Exs1(:); efld(mode+1:2*mode)=Eys1(:);
rs=[Rs,Rs]; rs=diag(rs);

%%%%%%%%%% Filling the matrices %%%%%%%%%%%%%%%

% Original resistivity is subtracted from the impedance matix.

Z=Z-rs;

for m=1:mode

   for n=1:mode

   argy=k*deltay*v(m)/2;
   argx=k*deltax*u(m)/2;
   sincx=1; sincy=1;
```

```
    if abs(argx)>1e-5, sincx=sin(argx)/argx; end;
    if abs(argy)>1e-5, sincy=sin(argy)/argy; end;
    expxy=exp(j*k*(xn(n)*u(m)+yn(n)*v(m)));

    fnm1(m,n)=expxy*sincx*sincy*deltax;
    fnm2(m,n)=expxy*sincx*sincy*deltay;

  end;

end;

% Filling the scattered matrix (First equation), and current
% coefficients, I.

FF1=pinv(fnm1); FF2=pinv(fnm2);
FFI=[FF1,zeros(mode,mode);zeros(mode,mode),FF2];

I=(efld*FFI.');

%%%%%%%%%%%% Matrix  Operations %%%%%%%%%%%%%

% Second equation (Equation 63) operations. Excitation vector V is from the
% data file.

ZIxy=Z*I.';

AA=V.'-ZIxy;

ZL=(AA./I.');

ZL1=real(ZL);

ZLx=(deltay/deltax).*ZL1(1:mode);
ZLy=(deltax/deltay).*ZL1(mode+1:2*mode);

% Reconstructed resistivity rx.

rx=reshape(ZLx,modex,modey);
rorg=reshape(Rs,modex,modey);
rx=rx-rorg;

uxx=reshape(uxx,modey,modex); vyy=reshape(vyy,modex,modey);
```

61

%%%%%%%%%% Plots %%%%%%%%%%%%%%%%%%%%%%%%%%%

% Plot of residue (rx) resistivity.

mesh(uxx',vyy,rx); grid; view(30,30);

%save s12 uxx vyy rx rorg
title('Comparision of the Resistivities; in x-direction');
xlabel('u'), ylabel('v'), zlabel('Resistivity Differences');

```
function [nu,nv]=dcsin(mode)

%%%%%%%%%%%%%%%%%%%%%%%%%%%%%%%%%%%%%%%%%%%%%%%%%%
% This function calculates the number of points inside the        %
% unit circle, and shows these points.                            %
%                                                                 %
% function [nu,nv]=dcsin(mode)                                    %
%                                                                 %
% Ugurcan Samli                                                   %
%%%%%%%%%%%%%%%%%%%%%%%%%%%%%%%%%%%%%%%%%%%%%%%%%%

% Area ratio of the unit circle and the total area.
tot_pts=1.28*mode;
totsqr=sqrt(tot_pts);

  if abs(round(totsqr)-totsqr)<0.2
    nu=round(totsqr);
    nv=round(totsqr);
  else
    nu=ceil(totsqr);
    nv=floor(totsqr);
  end;

[u,v]=center(nu,nv);

n_uv=nu*nv;
sintet=sqrt(u.^2+v.^2);

  for s=1:n_uv

    if sintet(s)>1
      u(s)=0;
      v(s)=0;
    else
      u(s)=u(s);
      v(s)=v(s);
    end;

  end;

aa=find(u==0);  bb=find(v==0);
```

63

```
u(aa)=[];  v(bb)=[];

[nu nv length(u) length(v)]

plot(u,v,'+'),xlabel('u'),ylabel('v'); axis([-1,1,-1,1]);
title('Points inside the unit circle');
```

```matlab
function [x,y]=center(modex,modey)

%%%%%%%%%%%%%%%%%%%%%%%%%%%%%%%%%%%%%%%%%%%%%%%%%%
%                    center.m                    %
% This Function finds the center points of the patches    %
% in the  Direction Cosine Space.                 %
%                                                 %
% [x,y]=center(modex,modey)                       %
%                                                 %
%                                                 %
% Ugurcan Samli, May, 1996.                       %
%%%%%%%%%%%%%%%%%%%%%%%%%%%%%%%%%%%%%%%%%%%%%%%%%%

Lx=2;  Ly=2;

deltax=Lx/modex; deltay=Ly/modey;

a=0;

for s=1:modey
 for ss=1:modex

  a=a+1;
  x(a)=(-Lx/2+deltax/4+(ss-1)*deltax);
  y(a)=(-Ly/2+deltay/4+(s-1)*deltay);

 end;
end;
```

65

```
%              green.m
% Ugurcan Samli, Resistive Plate MM solution
% This function computes the integral of green's function.

function gg=green(a,b,c,d,g,h,int);

w=0.225*h;

 if int==0
        r=sqrt(((b-a)^2+(c-d)^2)+w^2);
        gg1=exp(-2*j*pi*r)/r;
        gg=gg1*g/4/pi*g;
 end

 if int==2
        xg=[0.5773503 -0.5773503];
        ag(1:2)=[1,1];
 end

 if int~=0
        int2=int/2;
          for s=1:int2
                s1=int-s+1;
                ag(s1)=ag(s);
                xg(s1)=xg(s);
                xg(s)=-xg(s);
        end;

        xhigh=a+g/2;
        xlow=a-g/2;
        bb=(xhigh-xlow)/2;
        aa=(xhigh+xlow)/2;
        sum=0;

         for i=1:int
                x=bb*xg(i)+aa;
                r=sqrt((b-x)^2+(c-d)^2+w^2);
                sum=sum+ag(i)*exp(-j*2*pi*r)/r;
          end;
        gg=sum*bb/4/pi*g;
    end;
```

```
%              green1.m
% Ugurcan Samli, Resistive Plate MM solution
% This function computes the integral of green's function.

function gg=green1(a,b,c,d,g,h,int);

w=0.225*g;

 if int==0
        r=sqrt(((a-b)^2+(c-d)^2)+w^2);
        gg1=exp(-2*j*pi*r)/r;
        gg=gg1*h/4/pi/h;
 end;


 if int==2
        xg=[0.5773503 -0.5773503];
        ag(1:2)=[1,1];
 end;

 if int~=0
        yhigh=c+h/2;
        ylow=c-h/2;
        bb=(yhigh-ylow)/2;
        aa=(yhigh+ylow)/2;
        sum=0;
          for i=1:int
                y=bb*xg(i)+aa;
                r=sqrt((a-b)^2+(y-d)^2+w^2);
                sum=sum+ag(i)*exp(-j*2*pi*r)/r;
          end;
        gg=sum*bb/4/pi/h;
 end;
```

```
%               green2.m
% Ugurcan Samli, Resistive Plate MM solution
% This function computes the integral of green's function.

function gg=green2(a,b,c,d,g,h,int);

w=0.225*g;

  if int==0
        r=sqrt(((a-b)^2+(c-d)^2)+w^2);
        gg1=exp(-2*j*pi*r)/r;
        gg=gg1*h/4/pi/h;
  end;

  if int==2
        xg=[0.5773503 -0.5773503];
        ag(1:2)=[1,1];
  end;

  if int~=0
        int2=int/2;
                for s=1:int2
                  s1=int-s+1;
                  ag(s1)=ag(s);
                  xg(s1)=xg(s);
                  xg(s)=-xg(s);
                end;
        yhigh=c+h/2;
        ylow=c-h/2;
        bb=(yhigh-ylow)/2;
        aa=(yhigh+ylow)/2;
        sum=0;
         for i=1:int
                y=bb*xg(i)+aa;
                r=sqrt((a-b)^2+(y-d)^2+w^2);
                sum=sum+ag(i)*exp(-j*2*pi*r)/r;
         end;
        gg=sum*bb/4/pi/h;
  end;
```

```
%              green3.m
% Ugurcan Samli Resistive Plate MM solution
% This function computes the integral of green's function.

function gg=green3(a,b,c,d,g,h,int);

w=0.225*h;

 if int==0
       r=sqrt(((a-b)^2+(c-d)^2)+w^2);
       gg1=exp(-2*j*pi*r)/r;
       gg=gg1*g/4/pi/g;
 end;

 if int==2
       xg=[0.5773503 -0.5773503];
       ag(1:2)=[1,1];
 end;

 if int~=0
       int2=int/2;
        for s=1:int2
               s1=int-s+1;
               ag(s1)=ag(s);
               xg(s1)=xg(s);
               xg(s)=-xg(s);
         end;
       xhigh=a+g/2;
       xlow=a-g/2;
       bb=(xhigh-xlow)/2;
       aa=(xhigh+xlow)/2;
       sum=0;
        for i=1:int
               x=bb*xg(i)+aa;
               r=sqrt((x-b)^2+(c-d)^2+w^2);
               sum=sum+ag(i)*exp(-j*2*pi*r)/r;
         end;
       gg=sum*bb/4/pi/g;
 end;
```

```
%               green4.m
% Ugurcan Samli Resistive Plate MM solution
% This function computes the integral of green's function.

function gg=green4(a,b,c,d,g,h,int);

w=0.225*h;

 if int==0
        r=sqrt(((a-b)^2+(c-d)^2)+w^2);
        gg1=exp(-2*j*pi*r)/r;
        gg=gg1*g/4/pi/g;
end;

 if int==2
        xg=[0.5773503 -0.5773503];
        ag(1:2)=[1,1];
end;

 if int~=0
        int2=int/2;
         for s=1:int2
                s1=int-s+1;
                ag(s1)=ag(s);
                xg(s1)=xg(s);
                xg(s)=-xg(s);
          end;
        xhigh=a+g/2;
        xlow=a-g/2;
        bb=(xhigh-xlow)/2;
        aa=(xhigh+xlow)/2;
        sum=0;
         for i=1:int
                x=bb*xg(i)+aa;
                r=sqrt((x-b)^2+(c-d)^2+w^2);
                sum=sum+ag(i)*exp(-j*2*pi*r)/r;
          end;
        gg=sum*bb/4/pi/g;
  end;
```

```
%%%%%%%%%%%%%%%%%%%%%%%%%%%%%%%%%%%%%%%%%%%%%%%%%%%%%
%                                                   %
%                    sample.m                       %
%    This program analyses the frequency content of the E-field   %
%    in u and v directions.                         %
%                                                   %
%    Ugurcan Samli, August 96                       %
%                                                   %
%%%%%%%%%%%%%%%%%%%%%%%%%%%%%%%%%%%%%%%%%%%%%%%%%%%%%

clear all;
load b24.mat

Efld=Exs1;
Efld=reshape(Efld,modex1,modey1);

% fn : number of FFT points. k : Spatial Frequency index.
% us : Sampling interval in DCS.
% This is for bistatic case and normal incidence.

fn=128;

c1=0:fn-1;
us=2/(modex1-1);
k=c1*2/(fn*us);

% fft in 1-dimension. FFT is performed only in 1 column (or row).

k=k(1:fn/2+1);
e1=Efld(6,:);
e2=abs(fft(e1,fn));
figure(1);
plot(k,e2(1:fn/2+1)); grid;
xlabel('Number of samples in DCS');
ylabel('abs(fft)'); title('3 by 3 plate');

% fft in 2-dimension.

ff=abs(fft2(Efld,fn,fn));
[ku,kv]=meshgrid(k,k);
figure(2);
mesh(ku,kv,ff(1:fn/2+1,1:fn/2+1)), grid; view(30,30);
```

```
xlabel(' Number of Samples in u-direction');
ylabel('Number of Samples in v-direction'),
zlabel('abs(fft)'); title('3 by 3 plate');
```

LIST OF REFERENCES

1.   Faros, N. I., "Radar Cross Section Synthesis for Planar Resistive Surfaces," Master's Thesis, Naval Postgraduate School, 1994.

2.   Waddel, C. W., "Radar Cross Section Synthesis of Doubly Curved Surfaces," Master's Thesis, Naval Postgraduate School, 1995.

3.   David C. Jenn, *Radar and Laser Cross Section Engineering*, AIAA Education Series,Ohio, 1995.

4.   Balanis, A. C., *Advanced Engineering Electromagnetics*, John Wiley & Sons, Canada, 1989.

5.   "Survey of Numerical Electromagnetic Modeling Techniques," WWW Internet, University of Missouri, EMC Laboratory.

6.   Randy Bancroft, *Understanding Electromagnetic Scattering Using the Moment Method*, Artech House, Boston, 1996.

7.   D. C. Jenn, unpublished notes, Naval Postgraduate School, Monterey, CA.

8.   J. Moore and R. Pizer, *Moment Methods in Electromagnetics*, Research Studies Press, John Wiley & Sons Inc., June 1986.

INITIAL DISTRIBUTION LIST

		No. Copies
1.	Defense Technical Information Center 8725 John J. Kingman Rd., STE 0944 Ft. Belvoir, VA 22060-6218	2
2.	Dudley Knox Library Naval Postgraduate School 411 Dyer Rd. Monterey, California 93943-5101	2
3.	Professor David C. Jenn, Code EC/JN Department of Electrical and Computer Engineering Naval Postgraduate School Monterey, California 93943-5121	2
4.	Professor D. Curtis Schleher, Code EC/SC Department of Electrical and Computer Engineering Naval Postgraduate School Monterey, California 93943-5121	2
5.	Chairman, IW Academic Group Frederic H. Levien, Code EC/LV Naval Postgraduate School Monterey, California 93943	1
6.	Ltjg Uğurcan Şamlı Akmescit Sok. Ferah Apt. No : 1-11 Bakırköy-İstanbul Turkey	2
7.	Deniz Harp Okulu Komutanlığı Kütüphanesi Dz.H.O. Komutanlığı, Tuzla - İstanbul, 81704 Turkey	2
8.	Yıldızlar Suüstü Eüt. Mrk. Kom.'lığı Elektronik Harp Destek Merkezi Merkezi Kom.'lığı Gölcük - Kocaeli Turkey	1